Functional Coatings Prepared by Magnetron Sputtering for Innovative Applications

A. Fernández
Instituto de Ciencia de Materiales de Sevilla, CSIC-Univ. Sevilla

asuncion@icmse.csic.es
www.al-nanofunc.eu

LANE
Laboratorio Avanzado de Nanoscopías y Espectroscopías

CAPACITIES
AI-NANOFUNC
Advanced Laboratory for the NANO-Analisys of novel FUNCtional Materials

FP7-REGPOT- 285895

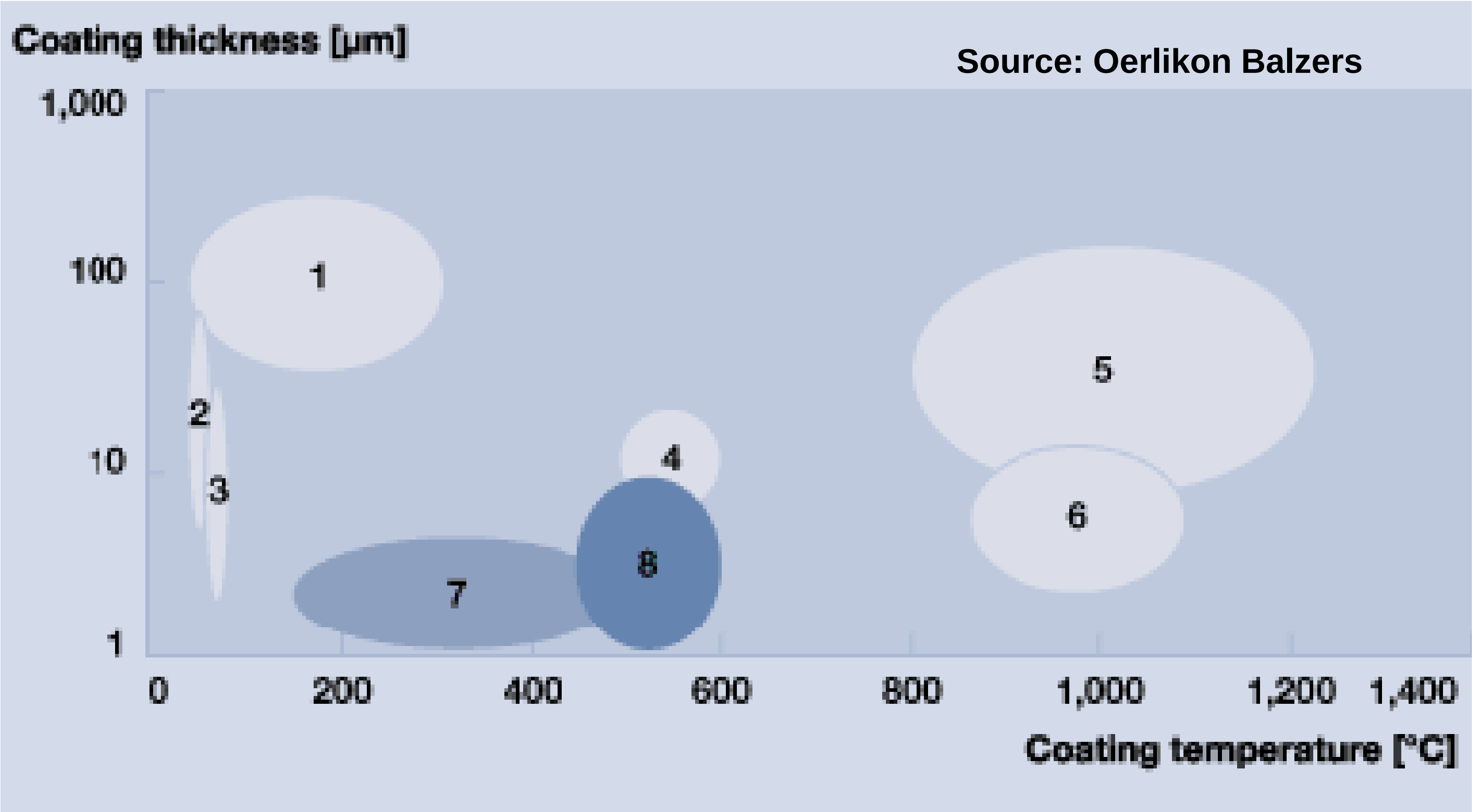

1.- Plasma spraying

2.-Electrolytic and chemical deposition; 3.-Phosphating

4.- Nitriding; 5.- Boronising

6.- CVD; 7.- PVD, PACVD

8.- P3e TM

PVD = Physical Vapour Deposition. Magnetron Sputtering.

PACVD = Plasma Assisted Chemical Vapour Deposition

P3eTM = Based on arc evaporation using pulse technology (Balzers)

Broad fields of applications – Broad fields of expertise

Coatings for mechanical parts applications: Hard & Super-hard, tribological and wear resistant. Protective coatings (corrosion)

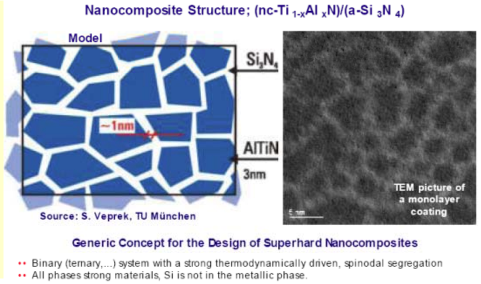

Nanocomposites nc-TiN / a-Si3N4

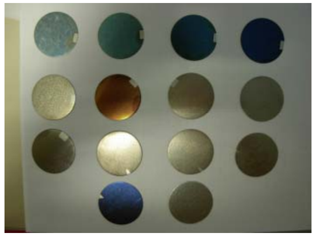

Interference colour

Cermet-based selective surfaces

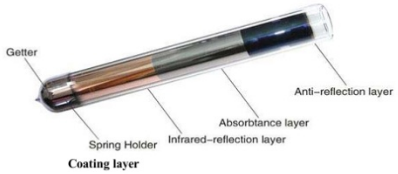

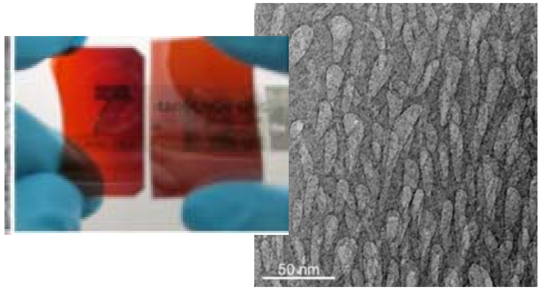

Porous a-Silicon

Optical coatings: Decorative, refraction index and reflectivity control. Cermet-based selective surfaces

Functional: Electrical and optical

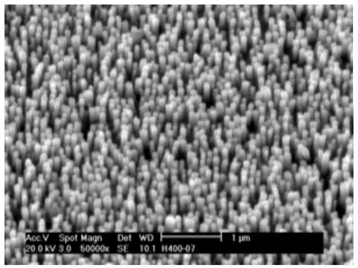

Thin film Photovoltaic

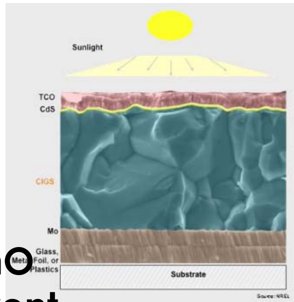

vertically aligned ZnO Nanowires. Transparent & conductive coatings

Catalytic coatings, self-cleaning

Co catalysts for H_2 generation

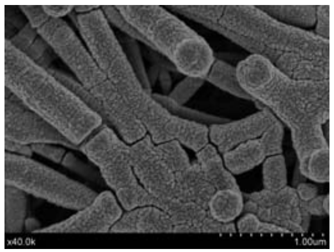

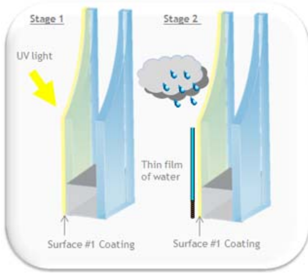

TiO2 based self-cleaning coating

Biocompatible & Bio-functional coatings

TiN, DLC, multi-component TiC, (Ti,Ta)C-based coatings

Coatings for mechanical parts applications: Hard & Super-hard, tribological and wear resistant. Protective coatings (corrosion)

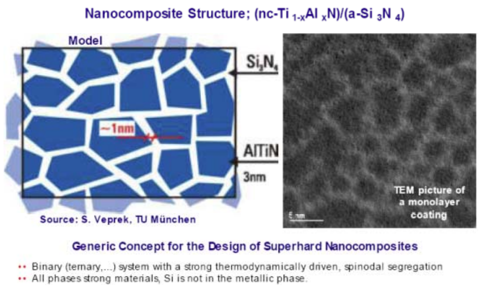

Nanocomposites
nc-TiN / a-Si3N4

Nanocrystalline materials. Bulk materials obtained for example by consolidation of nanometric powders or by ball milling. They contain nanocrystalline grains and a big amount of grain boundaries.

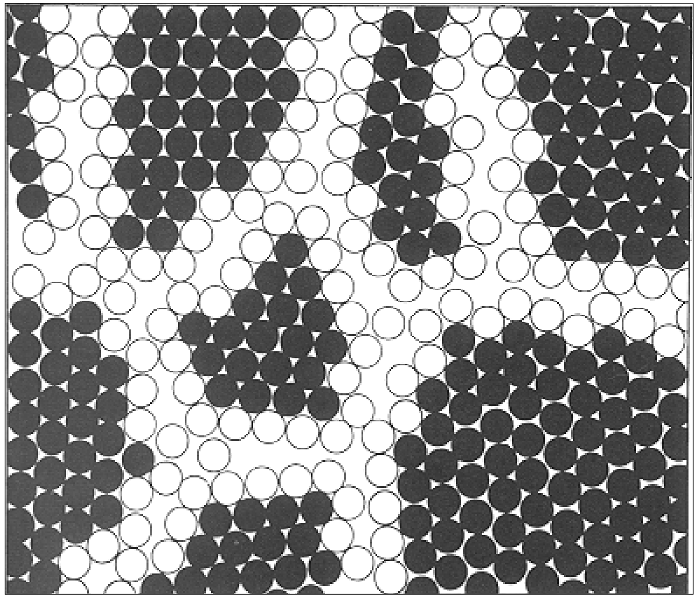

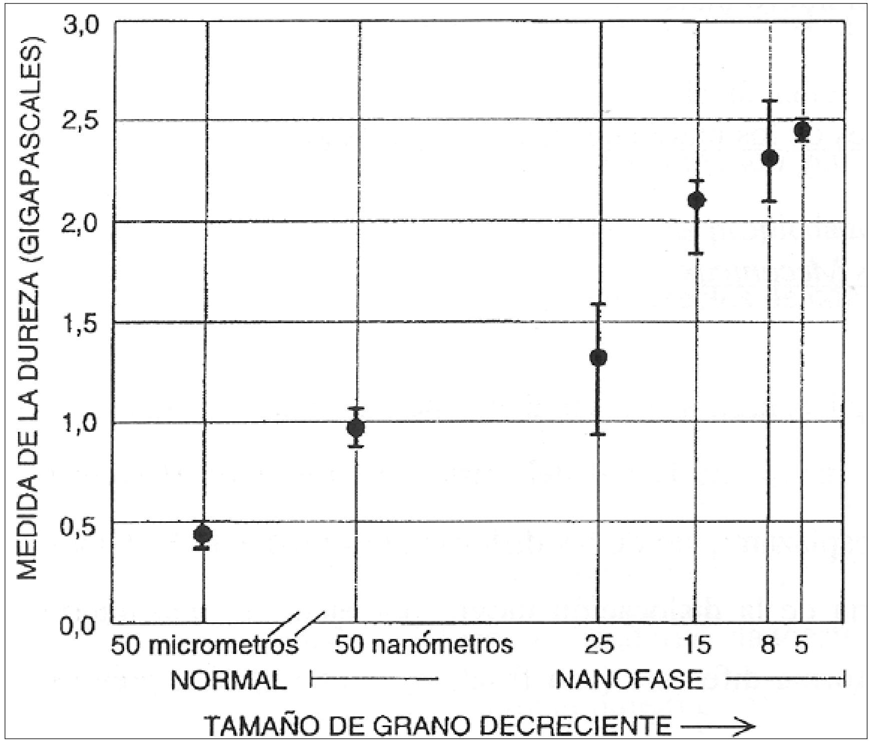

Hardness measurements for nanocrystalline copper as a function of grain size (6-50 nm). Comparison to a conventional Cu sample (50 μm grain sice).

Increase of hardness by reduction of grain size.

Polycrystalline materials

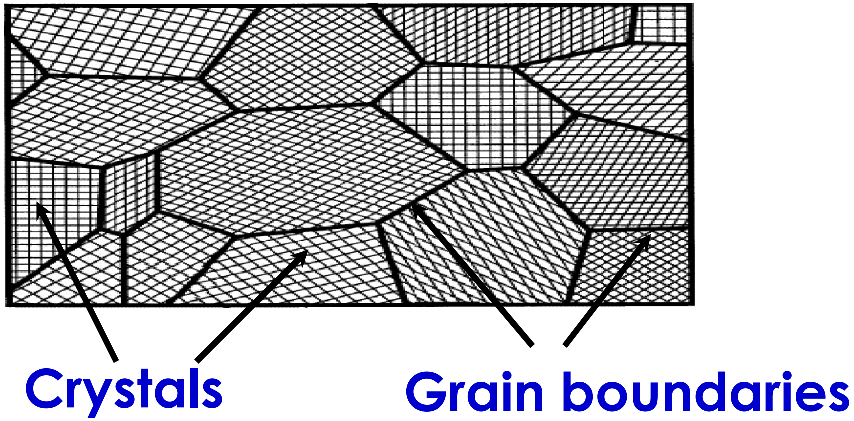

Hall-Petch effect

$$\sigma_c = \sigma_0 + \frac{k}{d^{1/2}}$$

Hardness (σ) increases as grain size (d) decreases. Dislocations are not propagated at grain boundaries. Deformation (i.e. indentation) produces dislocations that are stopped at the grain boundaries. The decrease in grain size produces an increase in the number of grain boundaries.

Reverse Hall-Petch effect.

The grain boundaries sliding produces propagation of dislocations

J. Schiotx, F.D. Di Tolla, K.W. Jacobsen, Nature, 391 (1998) 561

BUT: If d↓↓ ⇒ ↓ s_c

Sliding of grain boundaries appears

“Nanocomposite” hard coatings

Amorphous matrix
(ceramic, carbon, metal)

Nanocrystals (hard phase)
(nitrides, carbides, borides)

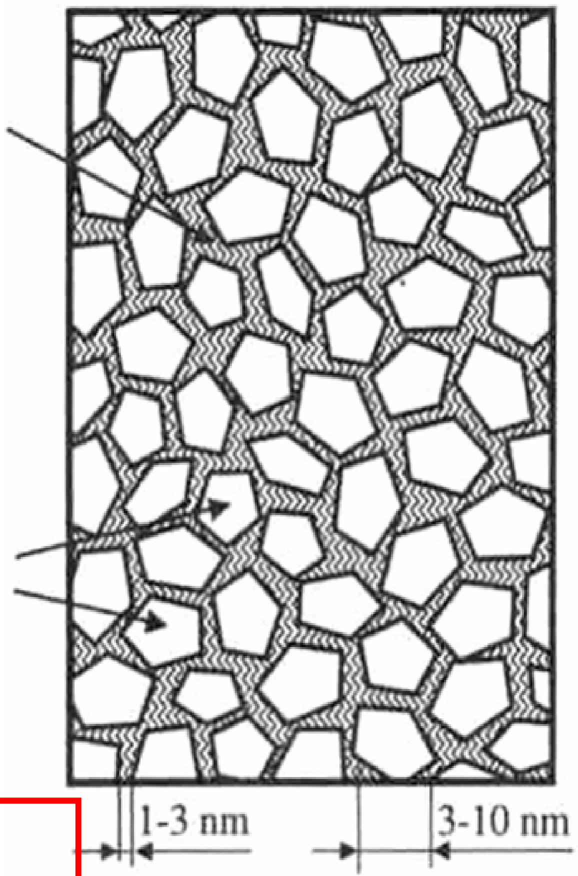

The amorphous phase avoid the grain boundaries sliding and hardness increases overcoming the reverse Hall-Pecht effect.

S. Vepřek, J. Vac. Sci. Technol. A 17 (1999) 2041

P. Nesládek & S. Vepřek, Phys. Stat. Sol. 177 (2000) 53

i.e. System: nc-TiN/a-Si_3N_4

S. Veprek, J. Vac. Sci. Technol. A 17 (1999) 2041
P. Nesládek & S. Veprek, Phys. Stat. Sol. 177 (2000) 53

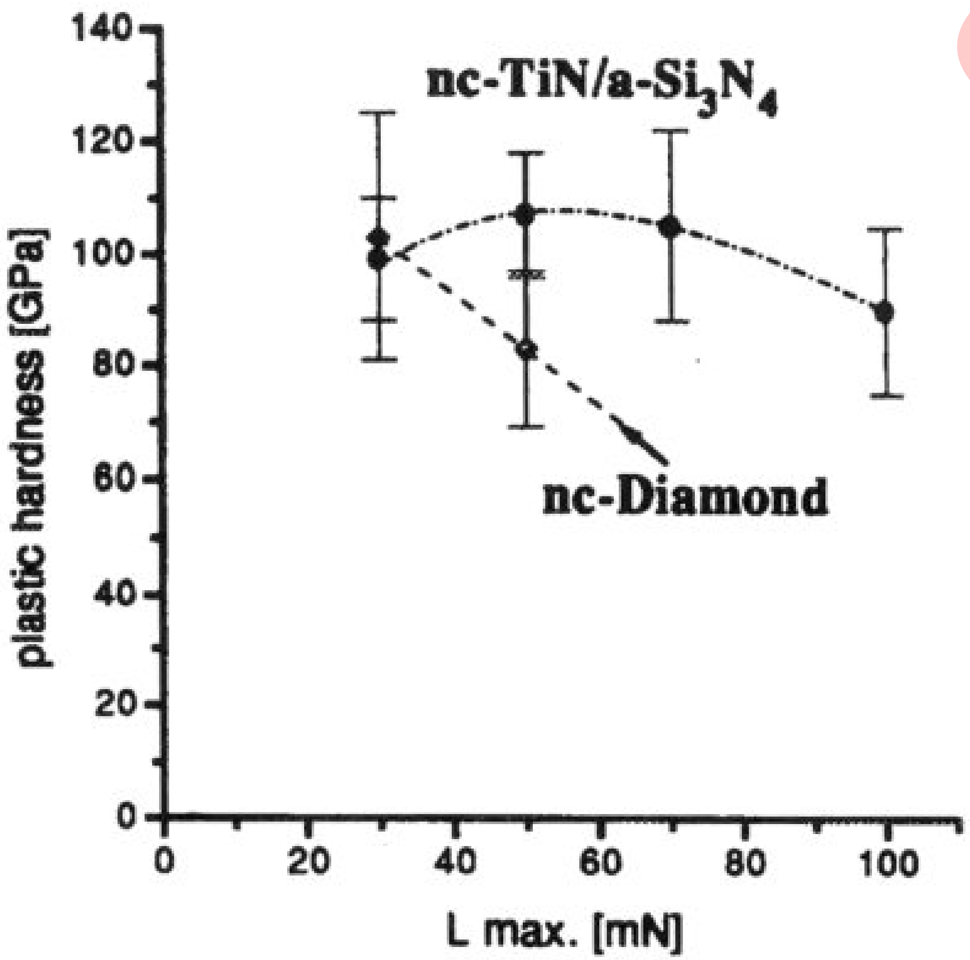

Hardness 40-90 GPa

Spinoidal phase segregation two immiscible materials completely segregate with sharp interfaces.

To avoid lattice misfit one of the phases should be amorphous

Nanocrystals (Ø =3-10 nm)
Amorphous matrix (t = 1-3 nm)

Superhard n-c:TiN/Si_3N_4 Coatings

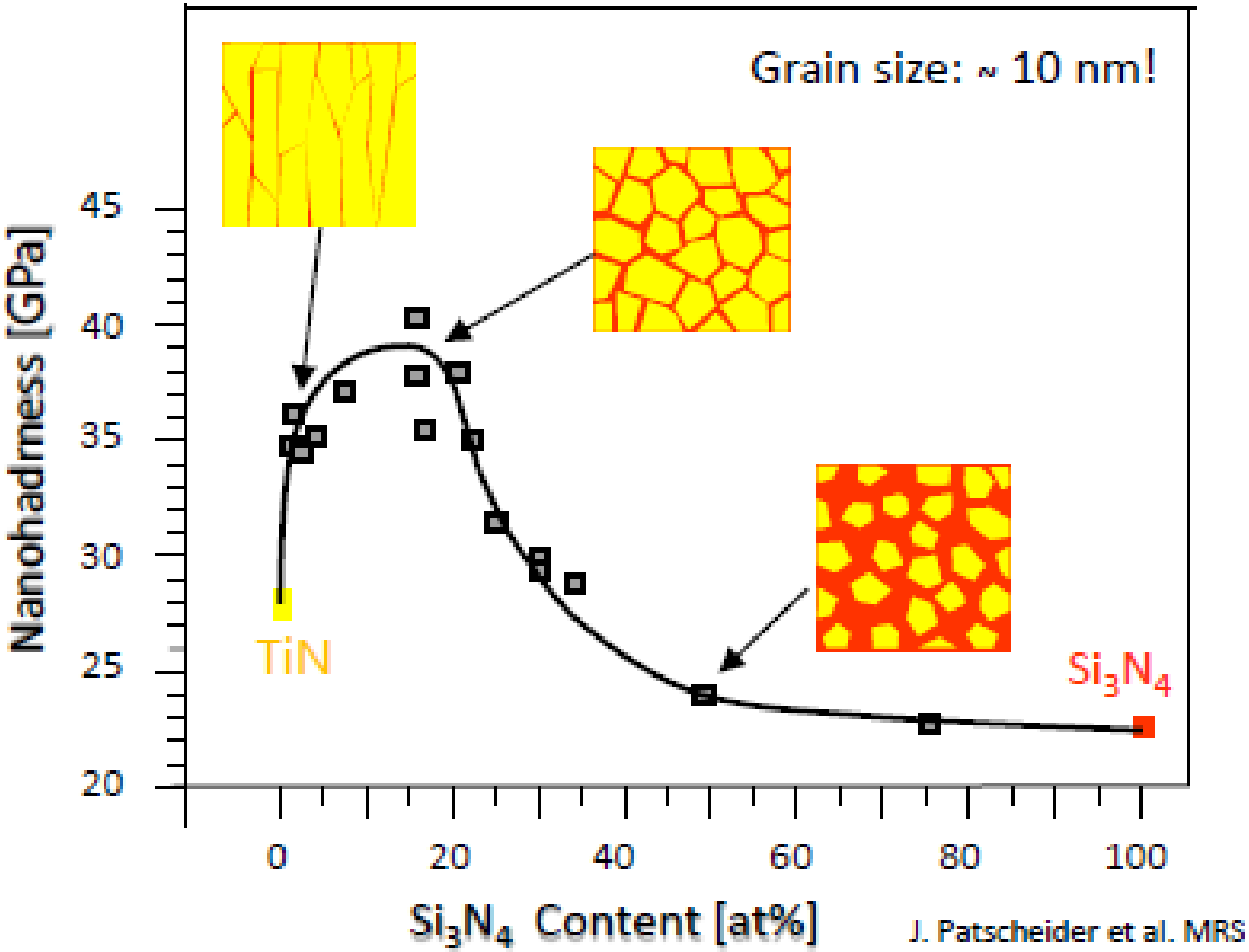

J. Patscheider et al. MRS Bulletin 28/3, 180 (2003), APL 96, 071908 (2010)

EMPA Materials Science & Technology

Multifunctional coatings.

"Nanocomposite" material which combine hardness with corrosion resistance. High speed machining. High temperatures working operation

- Coatings with a **nanocomposite microstructure:** nc-TiAlN/a-Si_3N_4 or nc-CrAlN/a-Si_3N_4

Nanocomposite

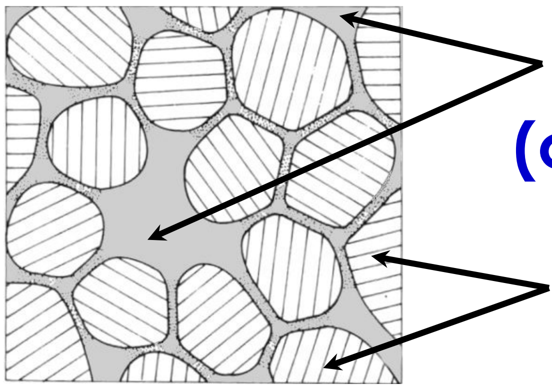

nc-$Ti_{1-x}Al_xN$/a-Si_yN_z

Composition & Microstructure → Properties

Role of impurities

Effect of dep. conditions

Oxygen incorporation

Localization

Effect of temperature

Morphology
Growth mode
Composition
Microstructure

Our approach: Magnetron sputtering with Ti-Al and Si tarjets. N_2 reactive plasma.

S. Veprek: Mainly vacuum arc approach.

The deposition chamber

- **"Magnetron Sputtering"**

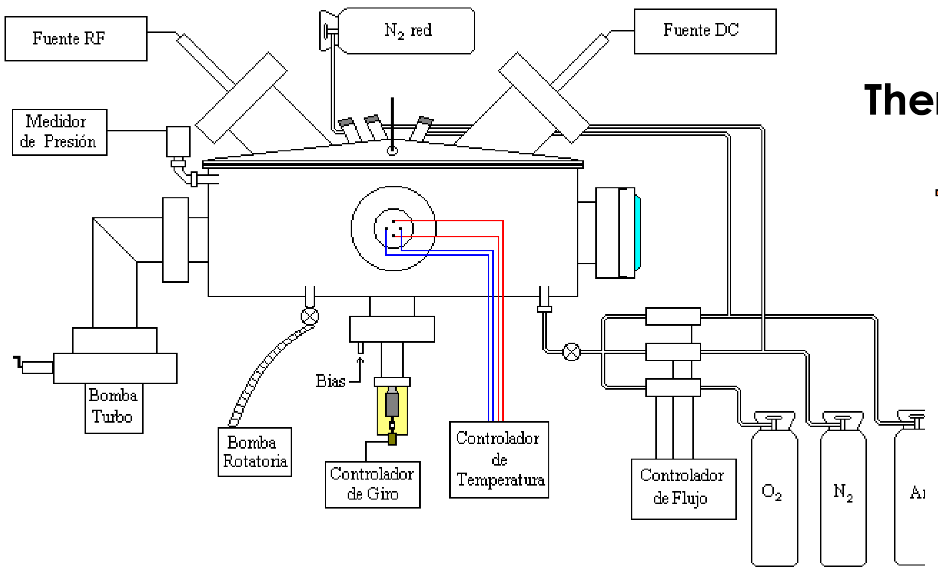

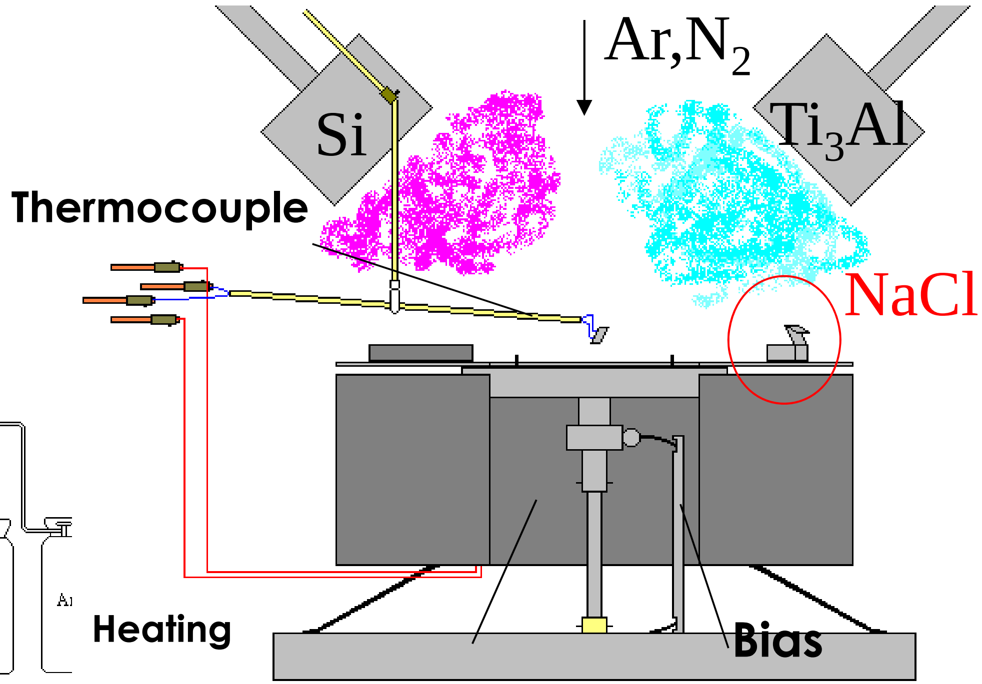

DC power supply: Up-to 1000W

RF power supply: Up-to 300W

Sample holder: Rotable, heatable, bias option.
Ti_3Al: 100-600 W DC; Si: 250 W RF
Bias: 0.25W in RF
Substrated temperature: 90°C and 300°C
Working pressure: 1.33 Pa N_2

TiAlSiN(O)/600-250/b-300ºC
Bias and high T improve reduction of oxygen cotent and favour spinoidal segregation

2-10 nm **crystals**

amorphous matrix 0.5-1.2 nm

2.1 , 2.4 , 1.5 Å

{200}, {111}, {202}

fcc TiN-based

Al if incorporated is occupying Ti positions in a non-ordered way

30 GPa. Substrate T 300ºC. Not a complete spinoidal phase segregation . Still too much amorphous phase

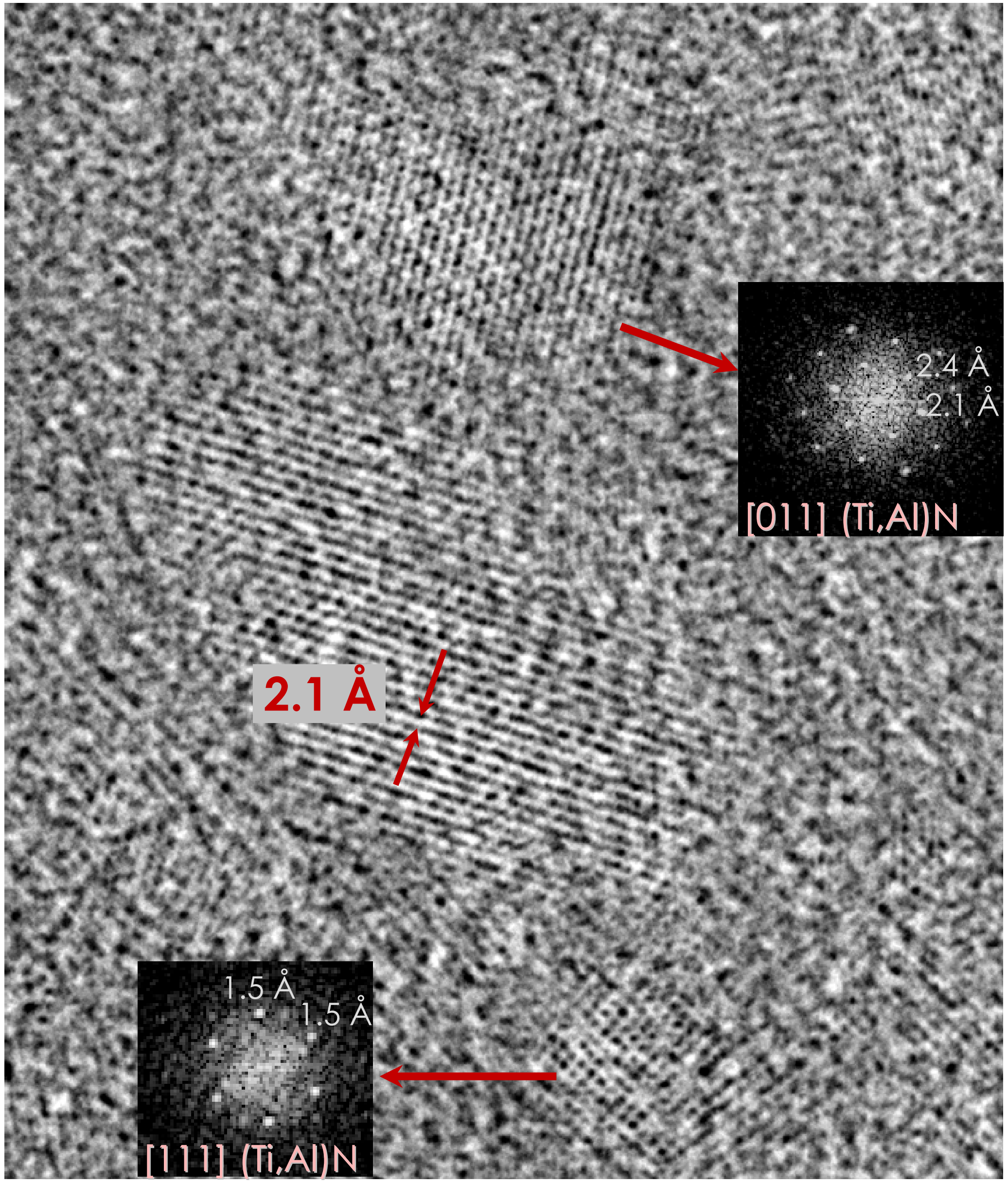

V.Godinho, T.C. Rojas, A. Fernández et al, Microscopy & Microanalysis 18, 2012, pp 568-581

TiAlSiN(O)/600-250
No bias and no high T
Columnar structure and higher Oxygen content

Electron Microscopy.
Energy Filtered TEM

White zones higher intensity of that element

Colunms are rich in:
Ti, Al, N

Interface area:
Si, O

Inner core rich in Si-O surrounded by Si-O-N

V.Godinho, T.C. Rojas, A. Fernández et al, Microscopy & Microanalysis 18, 2012, pp 568-581

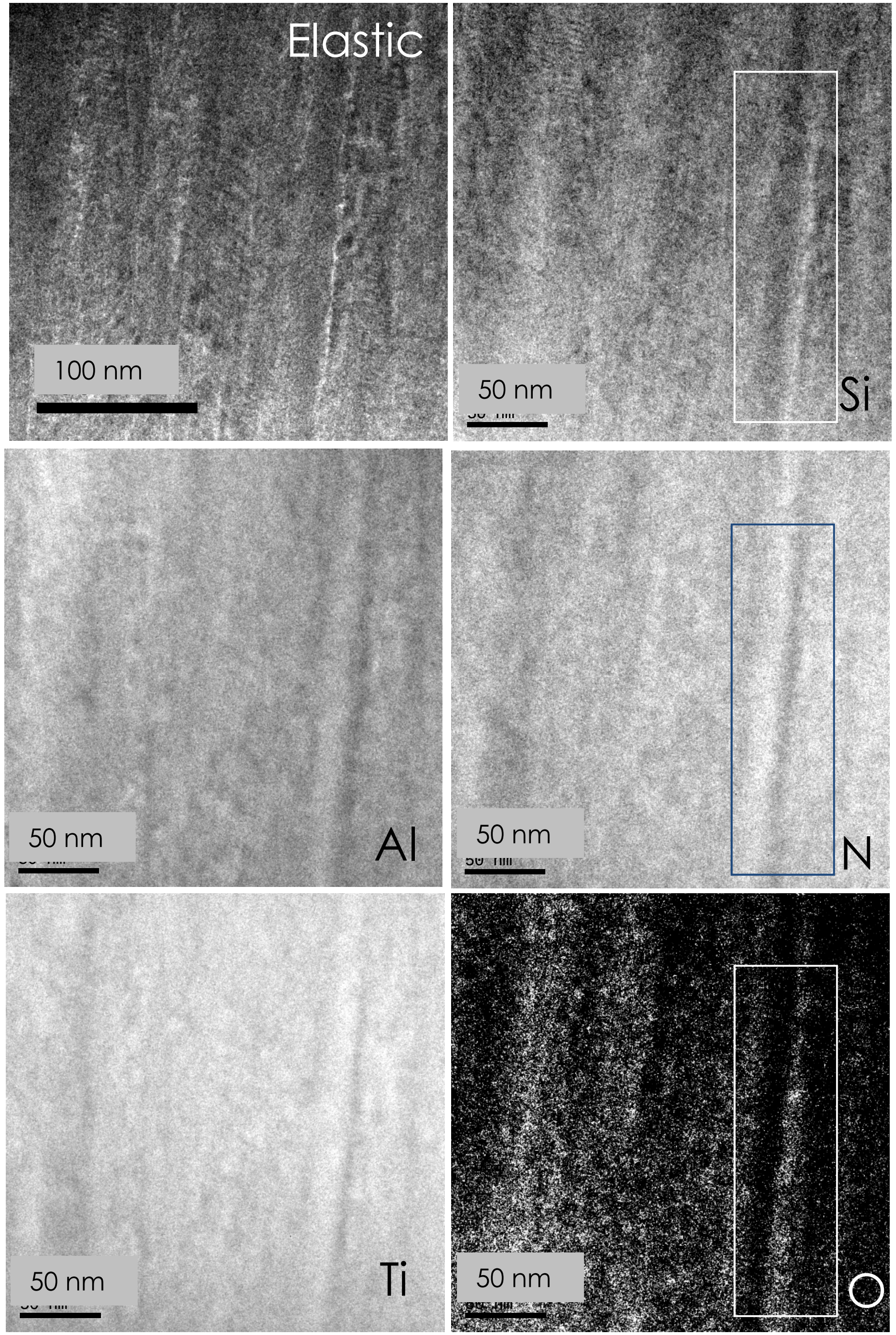

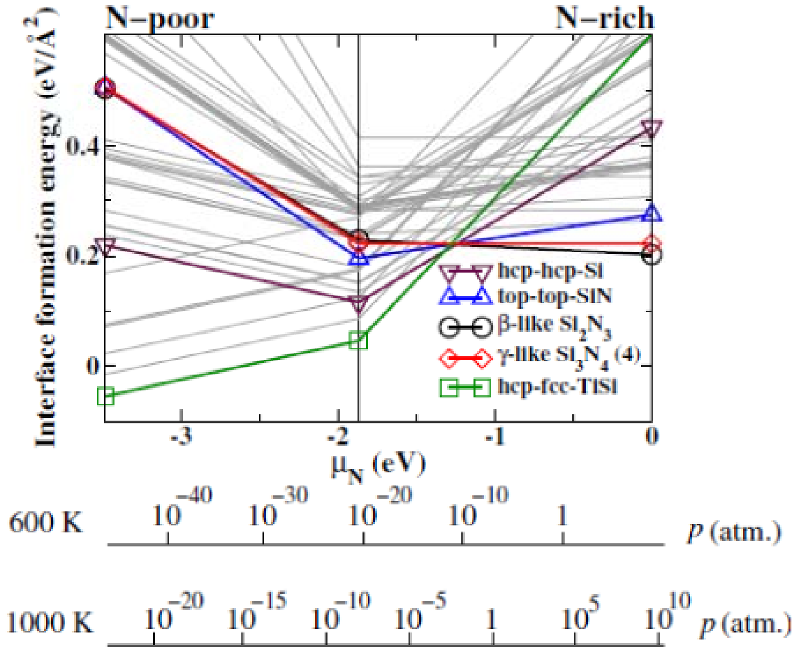

N-rich: β-like Si_2N_3

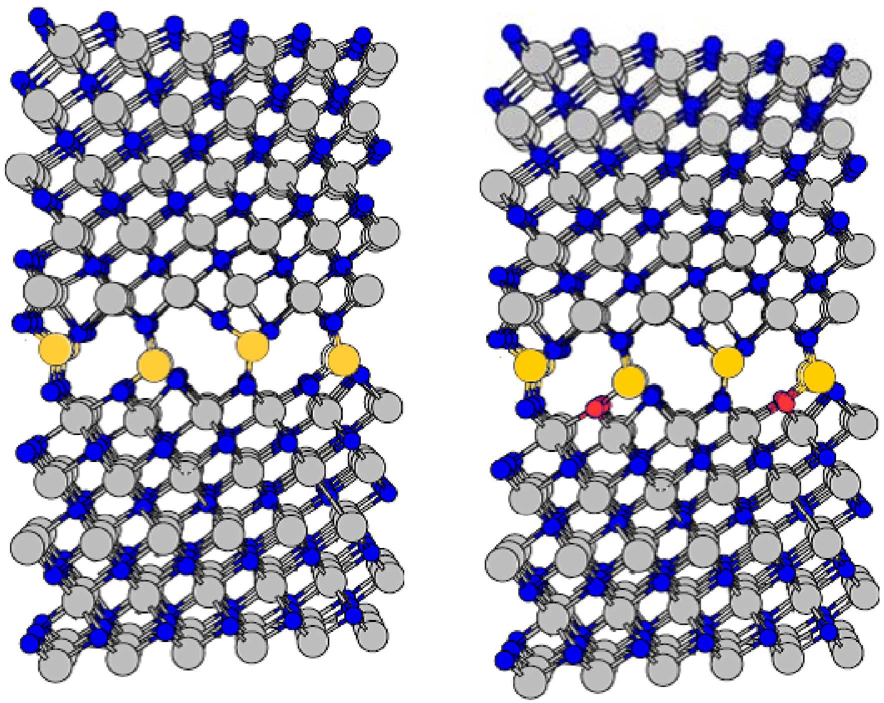

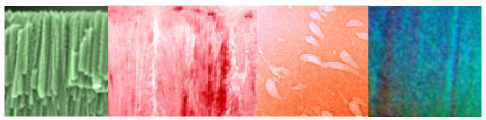

titanium silicon nitrogen oxygen

HAADF/STEM

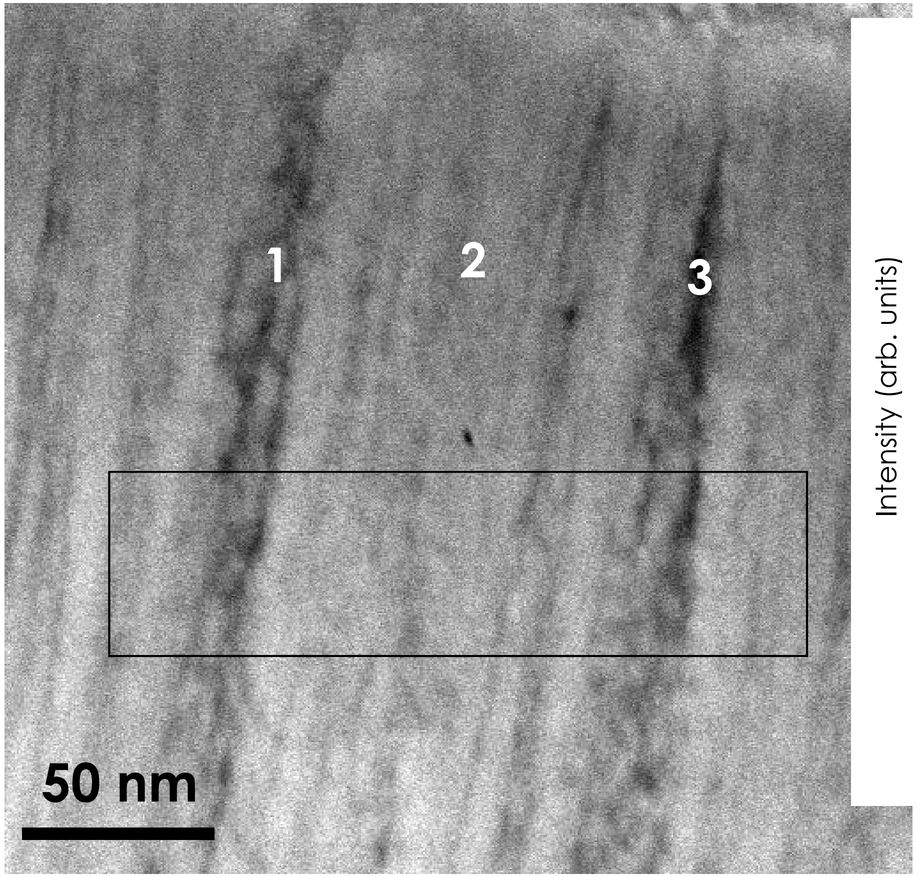

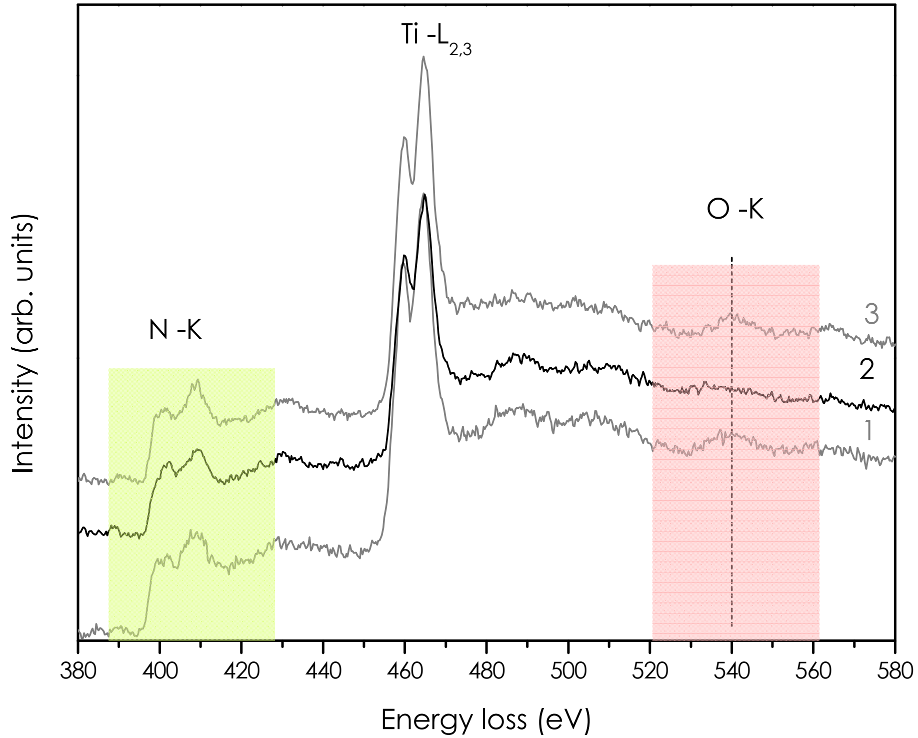

TiAlSiN(O)/600-250

N-O-Ti

V.Godinho, T.C. Rojas, A. Fernández et al, Microscopy & Microanalysis 18, 2012, pp 568-581

Multifunctional coatings.

“Nanocomposite” material in which the amorphous phase is a lubricant.

- Coatings with a **nanocomposite microstructure:** nc-TiC/a-C or nc-TiCN/a-CN_x a combination of hardness and low friction.

Nanocomposite

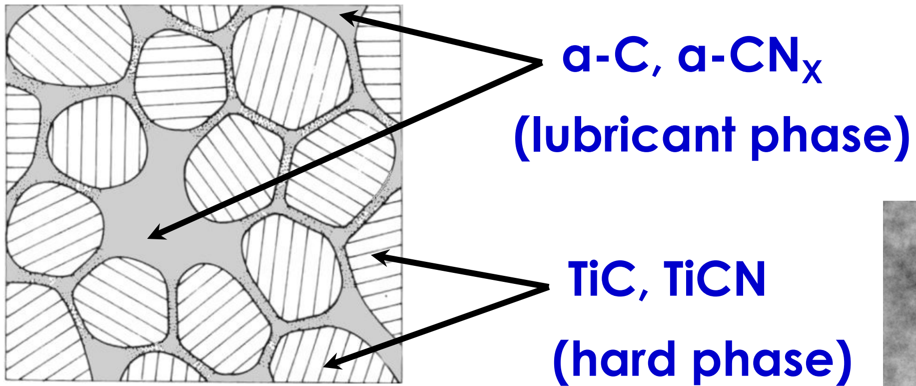

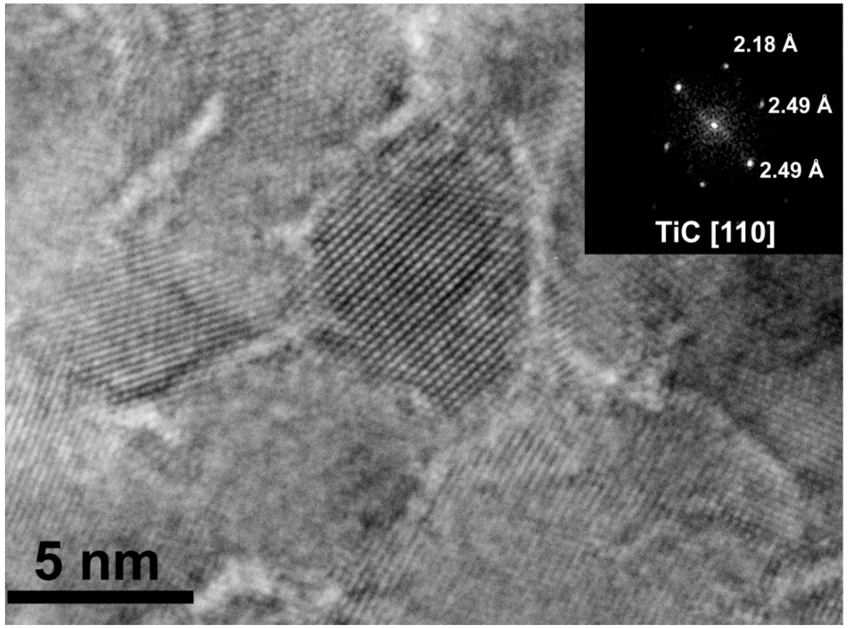

D.Martínez, A.Fernández, J.C.Sánchez-López et al., J.Vac.Sci.Tech.A, 23, 2005

Optical coatings: Decorative, refraction index and reflectivity control. Cermet-based selective surfaces

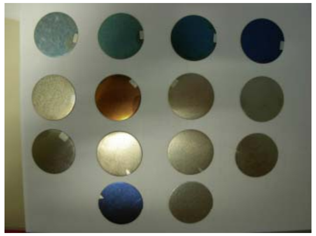

Interference colour

Cermet-based selective surfaces

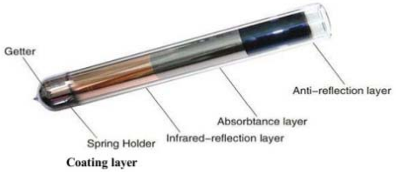

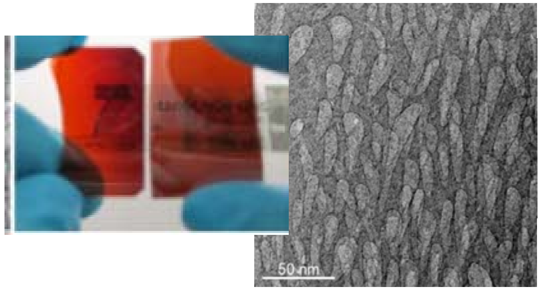

Porous a-Silicon

Interference coloured. **When the thickness of a coating is of the order of the wavelengths of the incident light,** the coating /substrate system can have remarkable reflective properties due to light wave interference and the difference in refractive index between the layer, the air, and the substrate. This effect, known as **thin-film interference,** can be used either on a single coatings or also in multilayered coatings.
More general periodic structures, not limited to planar layers, are known as **photonic crystals**.

When light moves from a medium of a given refractive index n_1 into a second medium with refractive index n_2, both reflection and refraction of the light may occur. **The Fresnel equations** describe what fraction of the light is reflected and what fraction is refracted (i.e., transmitted). They also describe the phase shift of the reflected light.

The light reflected from the upper and lower surfaces will interfere. The degree of constructive or destructive interference between the two light waves is dependent upon the difference in their phase. This difference is dependent upon **the thickness** of the film layer, **the refractive index** of the film, and **the angle of incidence** of the original wave on the film.

Structural colour

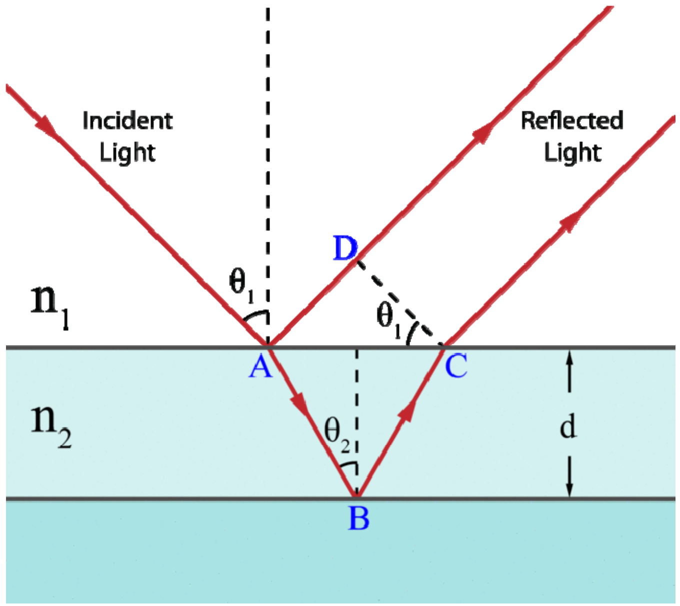

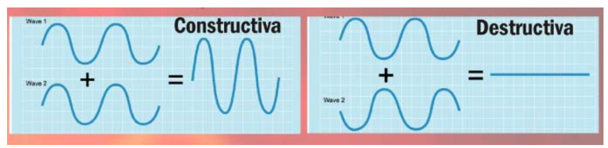

Magnetron sputtering provides a versatile method with a large selection of materials and excellent adhesion. Plastic covers with PVD coated with optical coating making optical, interference color effect.

(CenCorp Corporation)

Optical interference filter coatings produced by **Dual Magnetron Reactive Sputtering (DMRS) technology.**

(Omega Optical Inc.)

Intrinsically coloured. Amorphous **mixed oxide $M_xSi_yO_z$ thin films** (M: Fe, Ni, Co, Mo, W, Cu) for optical, coloring, and aesthetic applications. Specific colors can be selected by adjusting the plasma gas composition and the Si−M ratio in the magnetron target. M cations are randomly distributed within the SiO_2 amorphous matrix and that both the M concentration and its chemical state are the key parameters to control the final color of the films.

$M_xSi_yO_z$ thin films have been prepared by **reactive MS using a silicon target on which a series of metal strips have been arranged axially.**

Geometry: Substrates placed parallel to the magnetron.

Power: 100−300 W and pulsed DC voltage of 250−500 V at a frequency of 80 kHz.

Deposition pressure: 5.0×10^{-3} mbar.

Process gas: O_2/Ar mixtures with mass flow ratios from 0.05 to 2.5 depending on the type of thin film.

Coloured ceramic plates

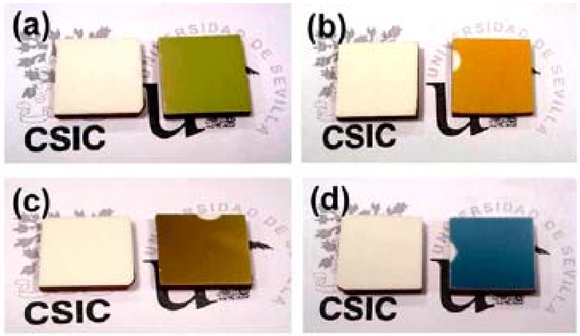

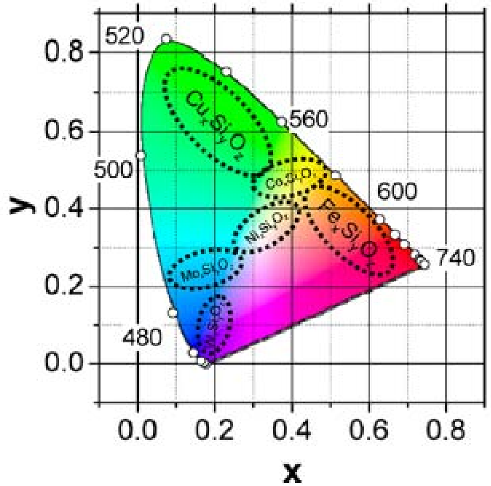

Colour coordinates diagram

Coloured polymeric ophtalmic lenses

dx.doi.org/10.1021/am302778h | ACS Appl. Mater. Interfaces 2013, 5, 1967−1976

J. Gil-Rostra, J. Chaboy, F. Yubero, A. Vilajoana, and A.R. González-Elipe

Light Absorbance / Reflection

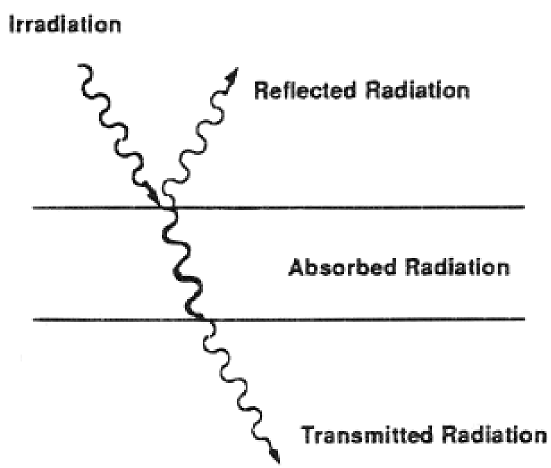

Solar absorptance. Solar radiation-absorption (*a*). The ratio of absorbed to incident radiation in the solar spectrum region.
Emittance, thermal infrared radiation-emission (ε). The energy radiated by the surface of a body per second per unit area

Kirchhoff's law recognized the experimental observation that a good absorber is a good emitter, and a poor absorber is a poor emitter. Naturally, a good reflector must be a poor absorber.

Black body, λ for which the intensity is maximal at a given T:

Wien's displacement law: $\mathbf{T.\lambda_{max} \approx 2.898x10^6}$

$T \rightarrow 523K$ ⇒ $\lambda \rightarrow 5.5\ \mu m$

$T \rightarrow 233K\text{-}373\ K$ ⇒ $\lambda \rightarrow 12.5\ \mu m - 8\ \mu m$

Dielectric Constant, Refractive Index. Reflectivity.
There is also a relation between optical and electrical properties in a material. For most naturally occurring materials at optical frequencies ***the dielectric constant*** *(ε)* is approximately the square of ***the refractive index*** (n^2).

High refractive index materials have in general high reflectivity in air.

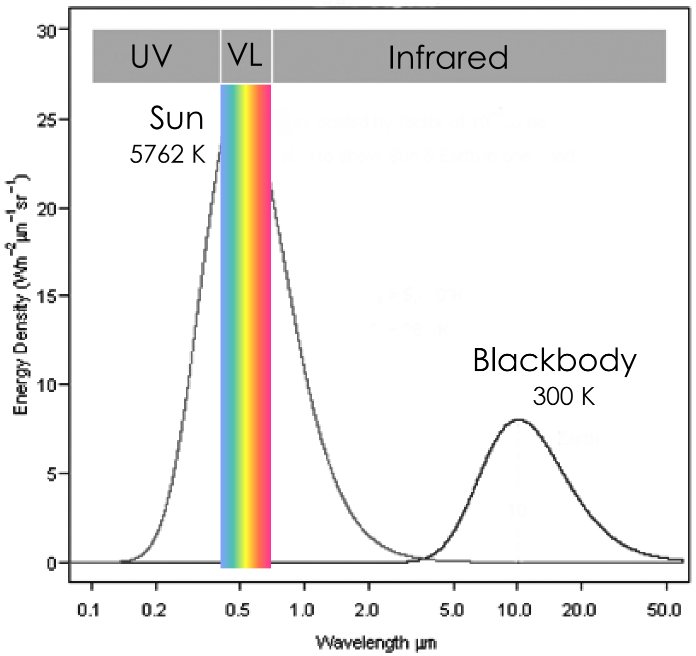

Solar absorptance

$$\alpha = \frac{\int_0^\infty \alpha_\lambda I_{\lambda,i} d\lambda}{\int_0^\infty I_{\lambda,i} d\lambda}$$

Thermal emittance

$$\varepsilon = \frac{\int_0^\infty \varepsilon_\lambda I_{\lambda b}(T) d\lambda}{\int_0^\infty I_{\lambda b}(T) d\lambda}$$

$I_{\lambda,i}$: incident spectral solar intensity
$I_{\lambda b}$: temperature-dependent spectral blackbody intensity

For opaque coatings

$$\varepsilon_\lambda = \alpha_\lambda = 1 - \rho_\lambda$$ Kirchhoff's law

Equilibrium temperature

$$T = 4\sqrt{\frac{S\alpha}{4\varepsilon\sigma}}$$

Stefan-Boltzmann's law

σ: Stefan-Boltzmann constant = 5.669×10^{-8} W.m^{-2}.K^{-4}

S: solar constant = 1353 W/m^2

Duffie & Beckmann, Solar Engineering of Thermal Processes, 1980

Selective surfaces

In solar thermal collectors, **a selective surface** or **selective absorber** is a means to increase its operation temperature and/or efficiency.

The selectivity is defined as the ratio of solar radiation-absorption (α) - to thermal infrared radiation-emission (ε).

Selective surfaces take advantage of the **different wavelengths range** of incident solar radiation and the emissive radiation from the absorbing surface:

Solar radiation covers approximately the wavelengths 350 nm - 4.000 nm (UV-A, visible and near infrared (NIR) or IRA+IRB).

Thermal infrared radiation, from materials with temperatures approximately in the interval -40 - 100°C, covers approximately the wavelengths 4.000 nm-40.000 nm = 4 um-.40 um. The thermal infrared radiation interval being named or covered by: MIR, LWIR or IR-C.

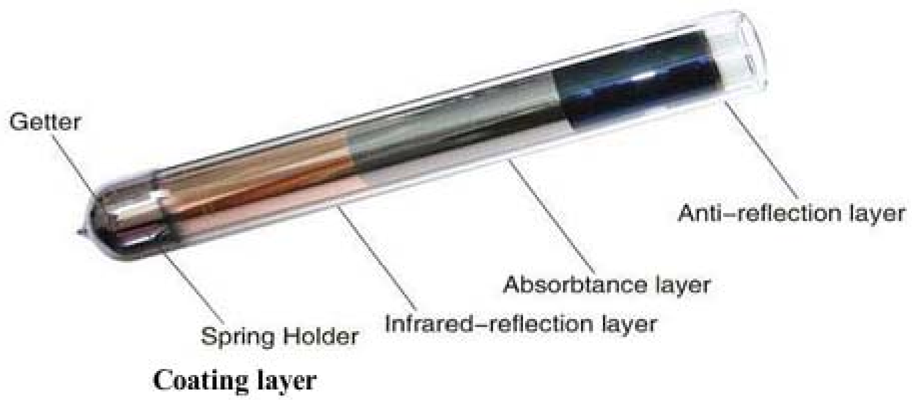

Maximize solar absorptance
&
Minimize thermal emission

http://www.physics.usyd.edu.au/app/solar/research/sputtering.html
The Solar Energy Group. University of Sydney

Selective surfaces

Anodic Solar absorbers. Magnetron sputtering based coatings (less environmental polluting than electrochemical coatings) based on DC reactive sputtering. Graded Al-N or Mo-Al_2O_3 cermet coatings based on conventional magnetron sputtering.

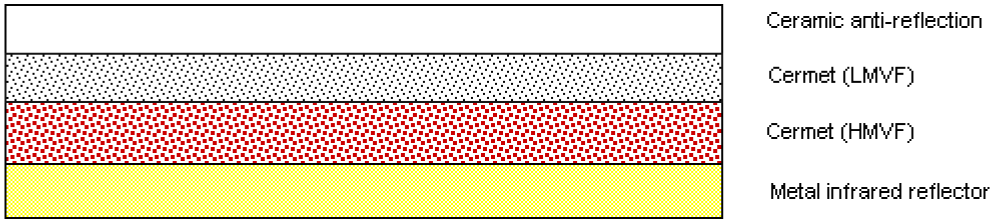

Fig.1. Schematic diagram of a solar selective absorber with double cermet layers, a low metal volume fraction (LMVF) cermet layer on a high metal volume fraction (HMVF) layer on a metal infrared reflector with a ceramic anti-reflection layer.

Highly absorbing coating in the VIS (black) and transparent in the IR

Cermet: Ceramic metal composites

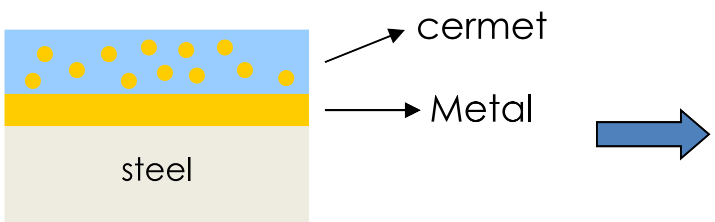

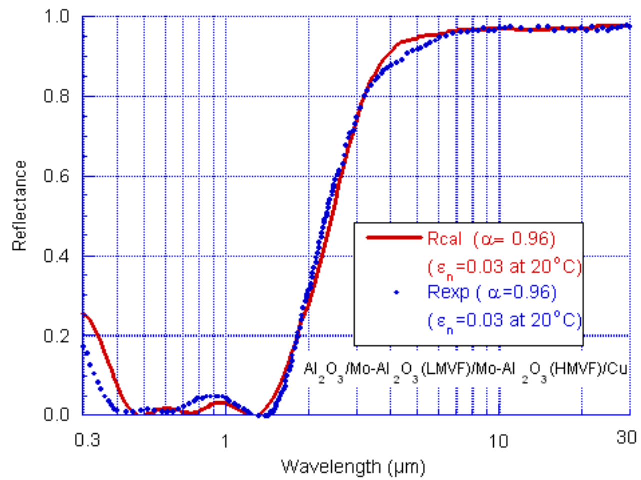

$Ti_{1-x}Al_xN(O)$ coatings with selective IR reflectivity

$Ti_{1-x}Al_xN$

TiN → AlN

metallic x dielectric

Changes in optical properties

IR reflectivity

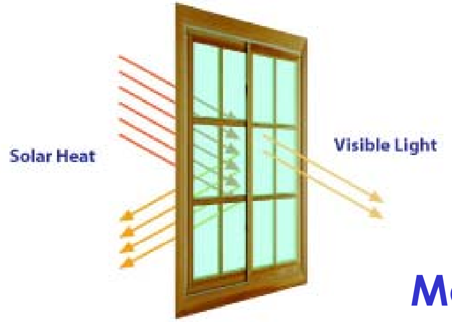

Solar-control windows

Maximize solar absorptance & Minimize thermal emission

Solar absorbers

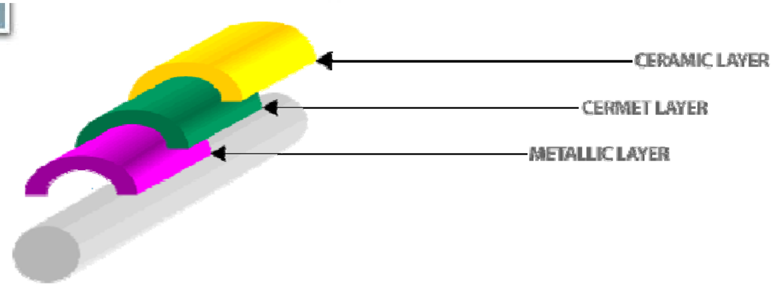

Satellite temperature control

Maximize solar absorptance & High thermal emission

V.Godinho, A.Fernández, et al. Solar Energy., 84, 2010, 1397- 1401.

PVD by reactive magnetron sputtering

Substrates:

AISI 316-R steel, ALUSI steel, Silicon (100), NaCl, Quartz and Glass

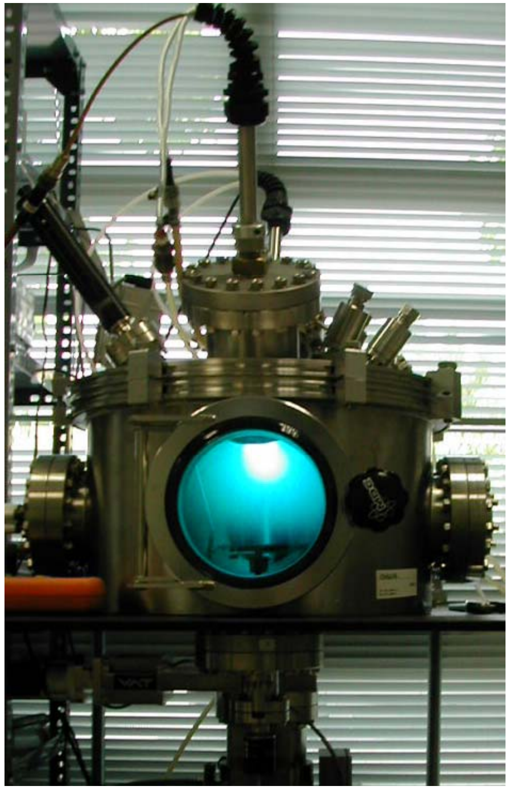

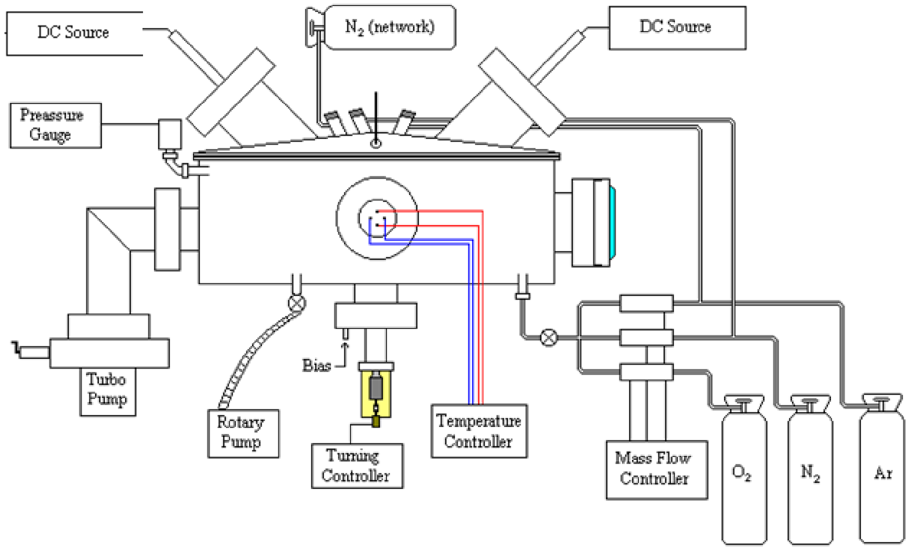

Pure Ti target, 99.995%

Pure Al target 99,9995%

N_2+Ar reactive gas

variable film composition

TiAlN coatings thickness

Sample	Ti	Al	%N2	t (min)	Profilometry	SEM fractography	Dep. rate (SEM)
TiAlN20	200	400	30	5	45 nm	60 nm	12 nm/min
TiAlN21	400	400	30	4	35 nm	80 nm	20 nm/min
TiAlN22	400	200	30	5	50-100 nm	75 nm	15 nm/min
TiAlN23	400	400	70	4	-	45 nm	11 nm/min
TiAlN24	400	400	15	4	100-140 nm	170 nm	42 nm/min
TiAlN25	200	400	15	5	80-120 nm	150 nm	30 nm/min
TiAlN26	600	400	15	4	140 nm	260 nm	65 nm/min
TiAlN27	400	600	15	5	135-230 nm	271 nm	54 nm/min
TiAlN28	200	600	15	5	105-170 nm	180 nm	36 nm/min
TiAlN29	400	200	15	5	-	235 nm	47 nm/min
TiAlN30	600	200	15	4	-	205 nm	51 nm/min
TiAlN31	600	600	15	3,5	-	202 nm	58 nm/min
TiAlN32	200	200	15	5	-	52 nm	10 nm/min

The deposition rate increases:

- by increasing the power supplied
- by decreasing the N2% ratio, the thickness decrease (TiAlN21, 23 and 24)

TiAlN coatings color

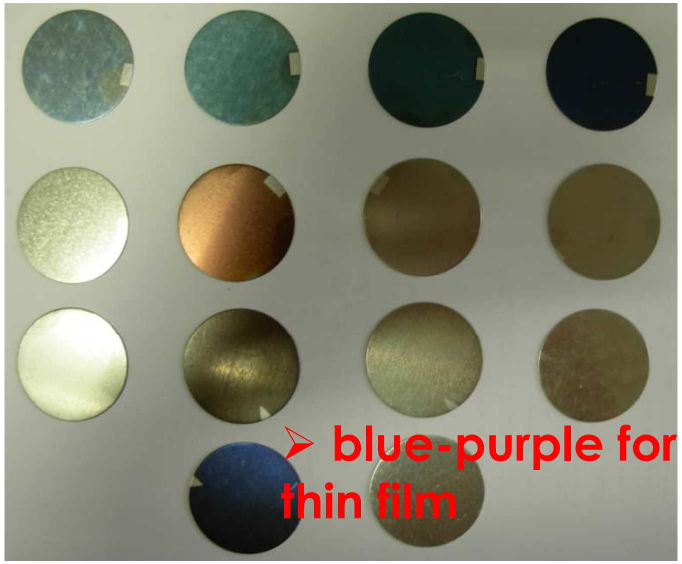

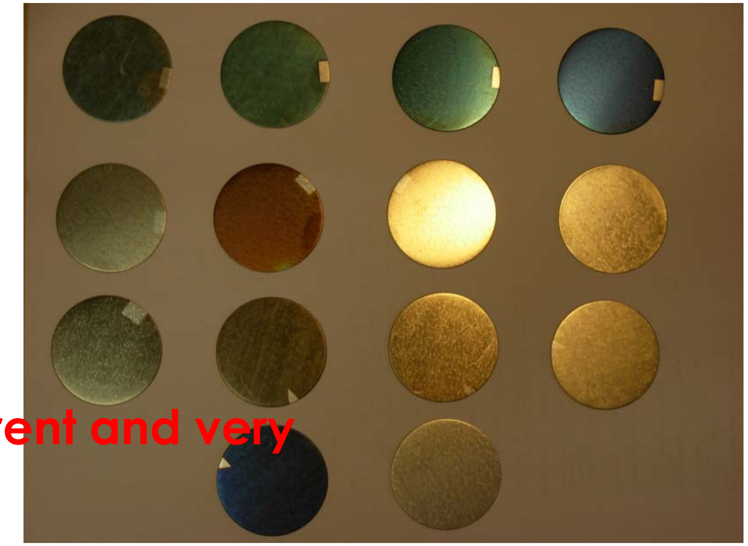

- blue-purple for transparent and very thin film
- grey-brown is the intrinsical colour

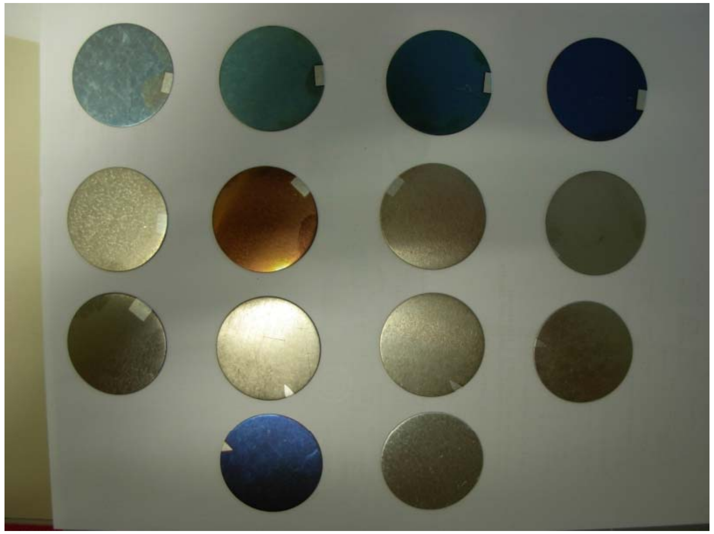

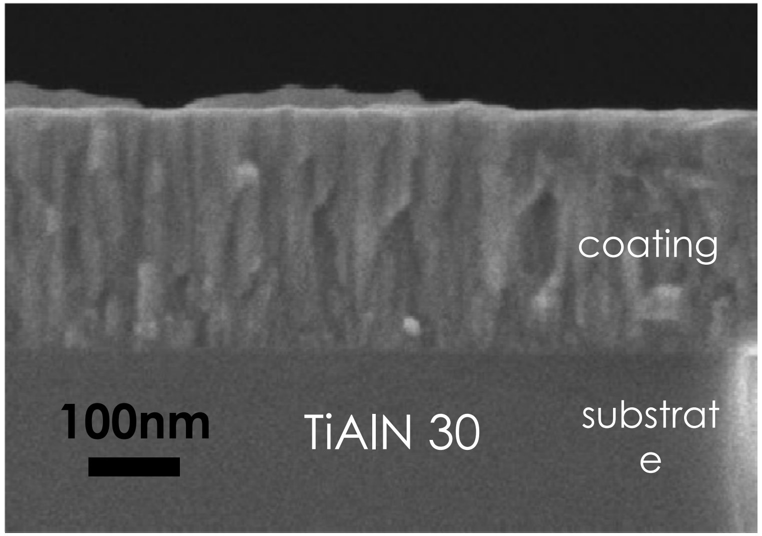

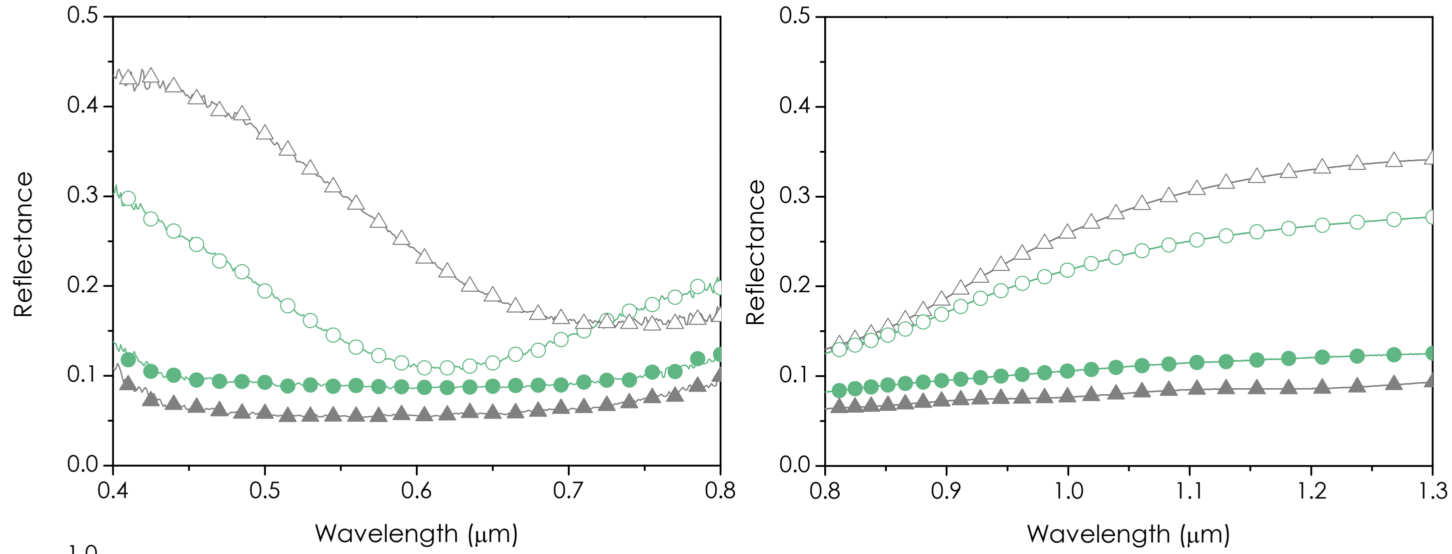

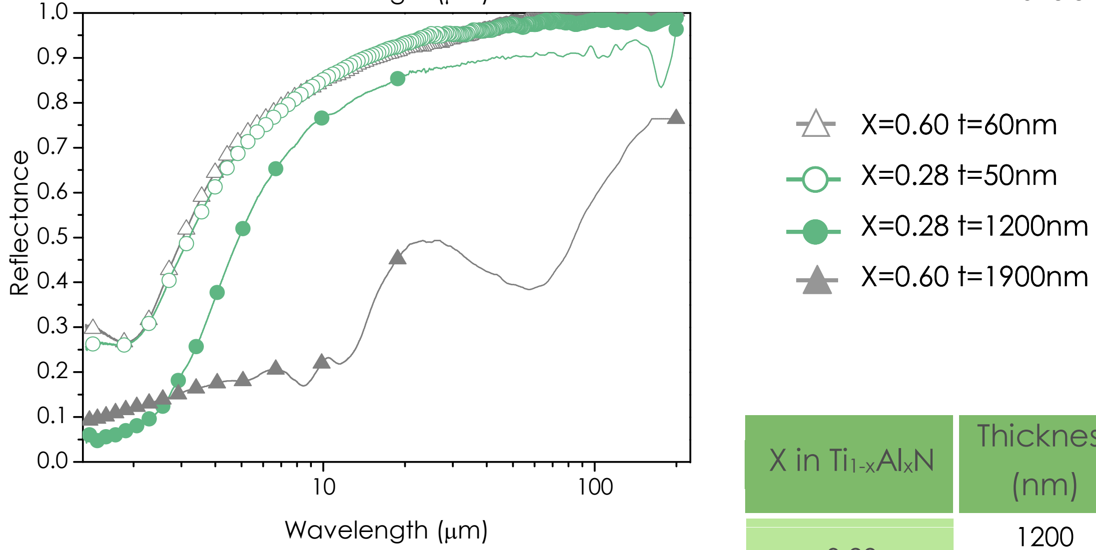

Solar absorbers

Satellite temperature control

X in $Ti_{1-x}Al_xN$	Thickness (nm)	α	ε	α/ε	Equilibrium temperature(°C)
0.28	1200	0.90	0.24	4.08	114
	50	0.84	0.15	5.40	150
0.60	1900	0.93	0.72	1.29	24
	60	0.79	0.15	5.00	142

Reflectance Spectra

V.Godinho, A.Fernández, et al.
Solar Energy., 84, 2010, 1397- 1401.

Porous silicon

Photonic devices

Microelectronics

Solar energy conversion

Up to now

1 Commonly produced by electrochemical methods

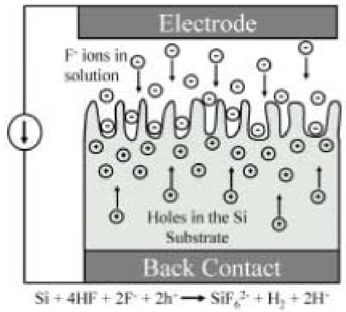

Changing electrolyte concentration and current, different structures are obtained

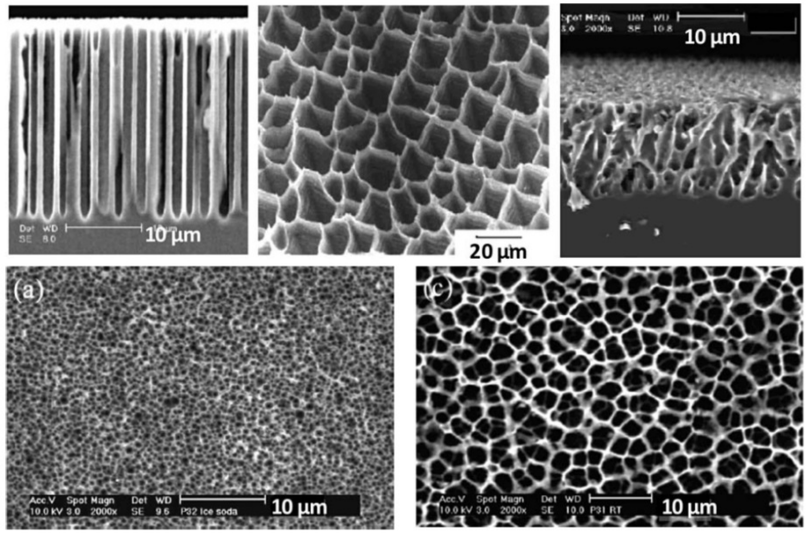

G.Korotcenkov, B.K. Cho
Silicon porosification:State of the Art
Critical Reviews in Solid State Materials Sciences, 35(2010)153-260

2 Transfer to less expensive substrates

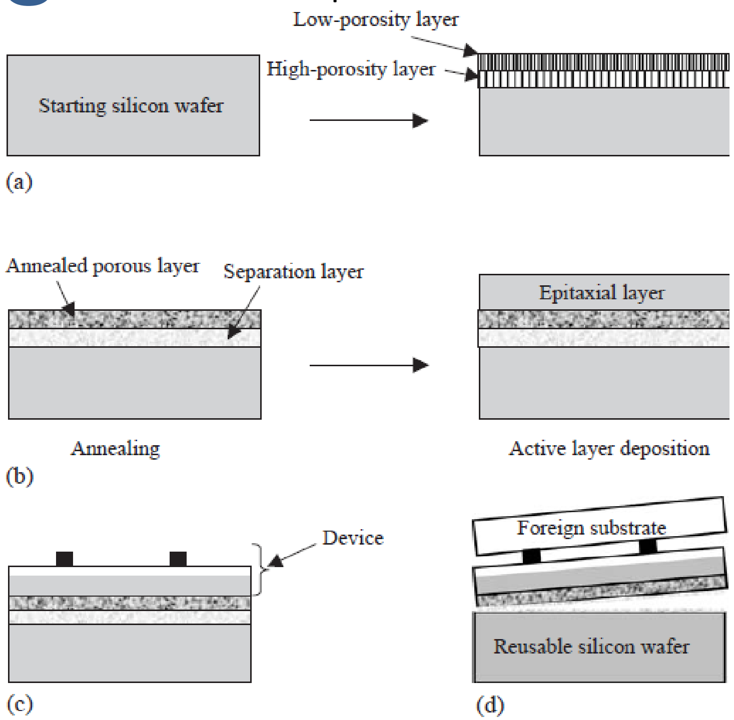

C.S. Solanki, R.R. Bilyalov, J. Poortmans, J. Nijsw, R. Mertens
Porous silicon layer transfer processes
for solar cells, Solar Energy Materials & Solar Cells 83 (2004) 101–113

New method
Control of the micostructure in the Nanoscale

OPEN ACCESS
IOP PUBLISHING NANOTECHNOLOGY
Nanotechnology 24 (2013) 275604 (10pp) doi:10.1088/0957-4484/24/27/275604

A new bottom-up methodology to produce silicon layers with a closed porosity nanostructure and reduced refractive index

V Godinho[1], J Caballero-Hernández[1], D Jamon[2,3], T C Rojas[1], R Shierholz[1], J García-López[4], F J Ferrer[4] and A Fernández[1]

magnetron sputtering
150W rf
He atmosphere

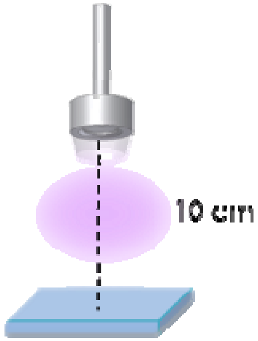

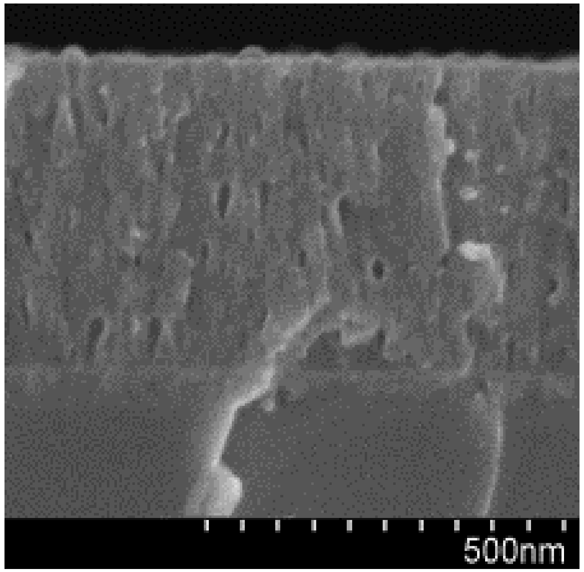

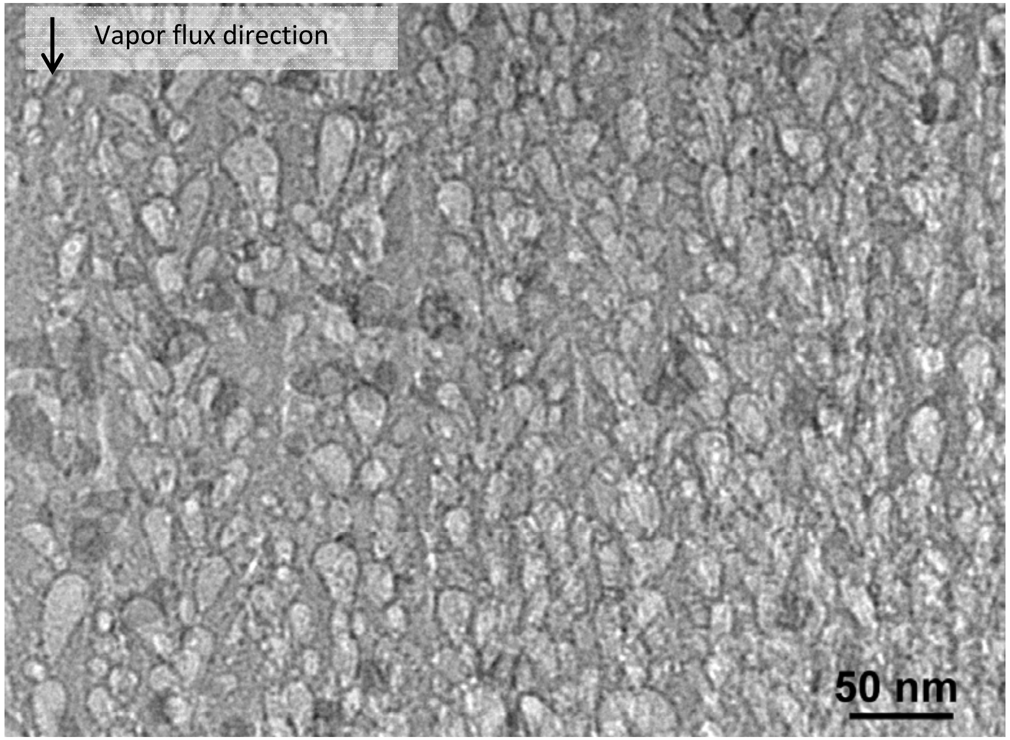

Porous Si coatings deposited by magnetron sputtering

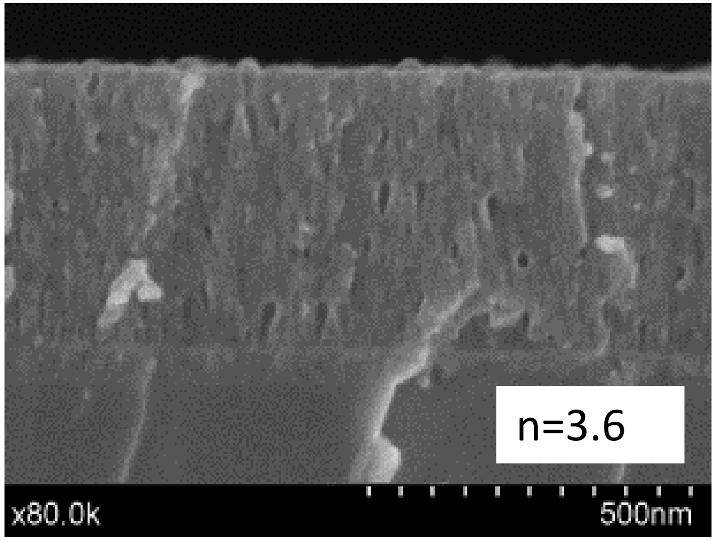

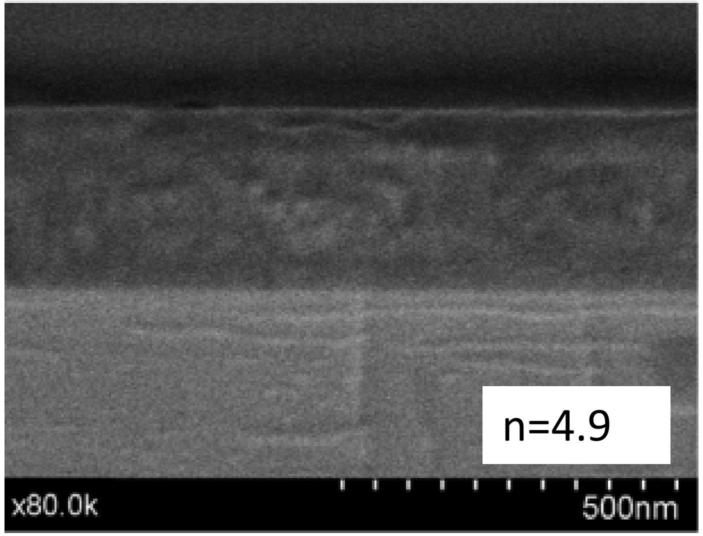

material	n_{500nm}
c-Si	3.49
a-Si	4.90
PSi	3.5-1

- Handbook of Optics, 3rd edition, Vol. 4. McGraw-Hill 2009

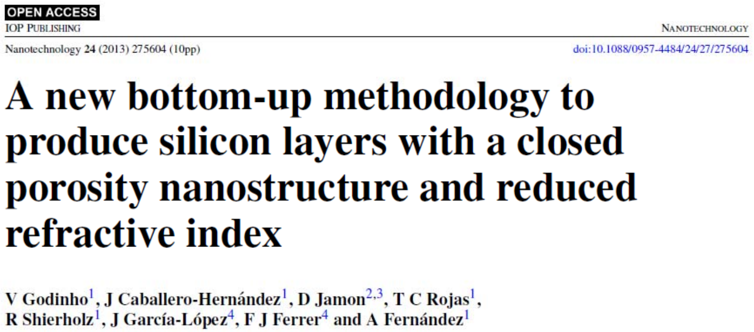

OPEN ACCESS
IOP PUBLISHING NANOTECHNOLOGY
Nanotechnology 24 (2013) 275604 (10pp) doi:10.1088/0957-4484/24/27/275604

A new bottom-up methodology to produce silicon layers with a closed porosity nanostructure and reduced refractive index

V Godinho[1], J Caballero-Hernández[1], D Jamon[2,3], T C Rojas[1], R Shierholz[1], J García-López[4], F J Ferrer[4] and A Fernández[1]

Pores oriented in magnetron direction

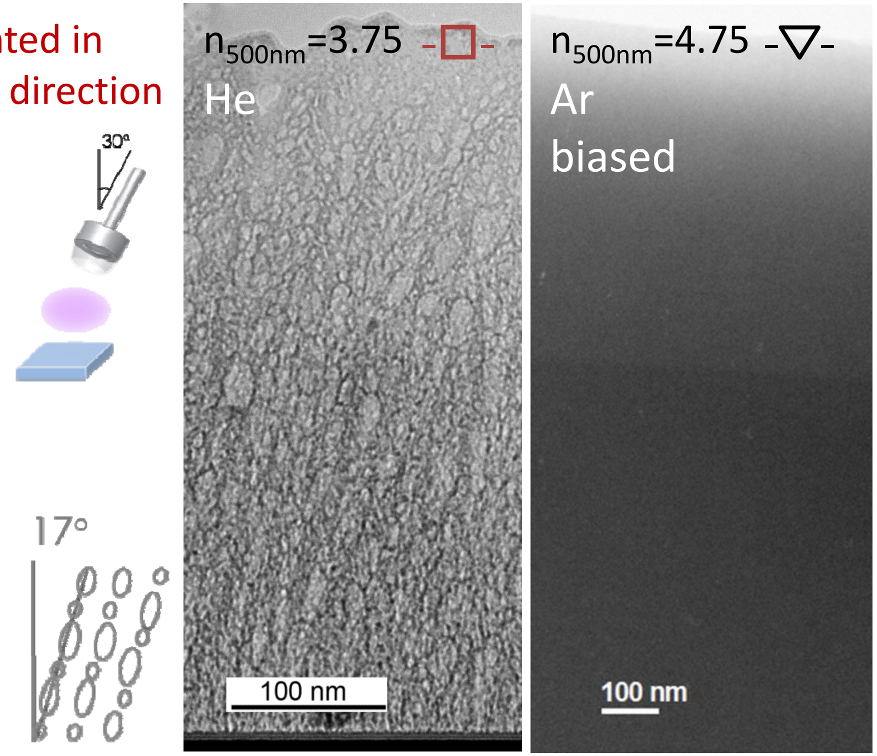

Pore size increases with increase of power

50W -○-   150W -□-

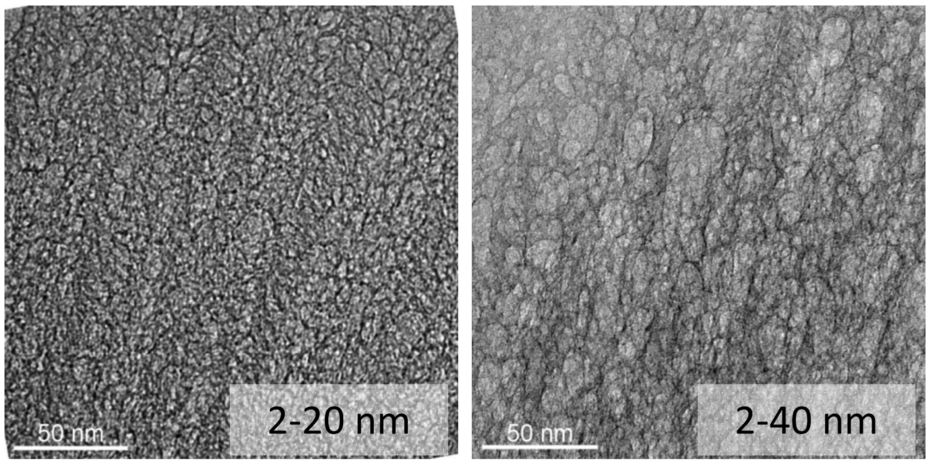

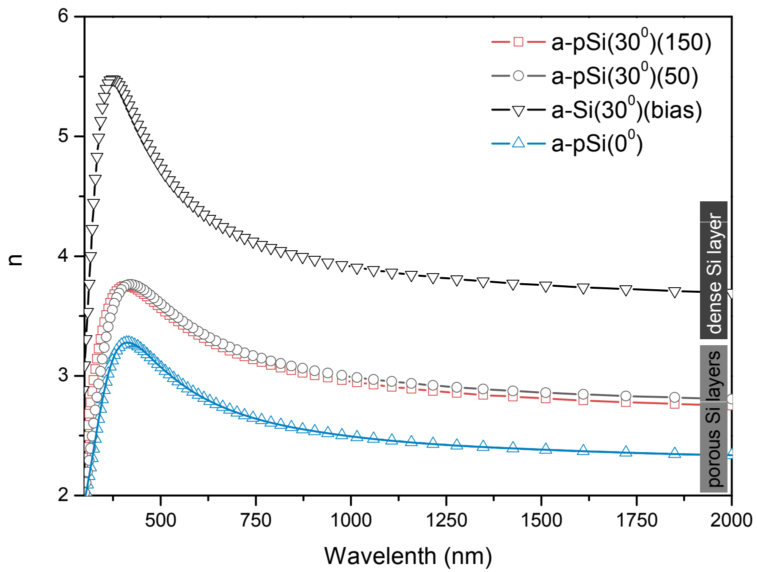

p-RBS measurements were performed with 1.7 MeV protons and a solid state detector located at 165° scattering angle

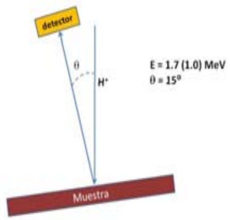

Porous coating

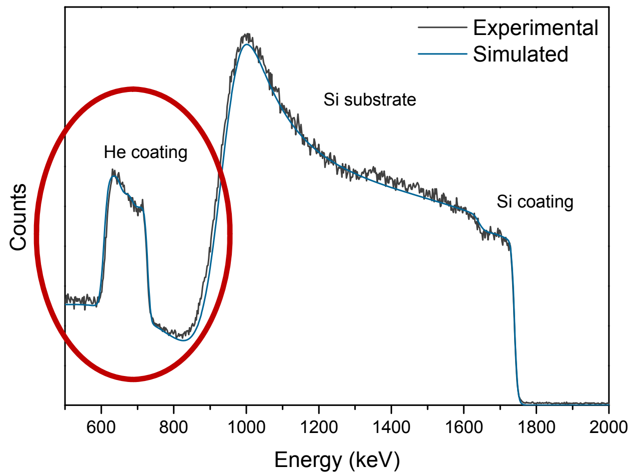

dense coating

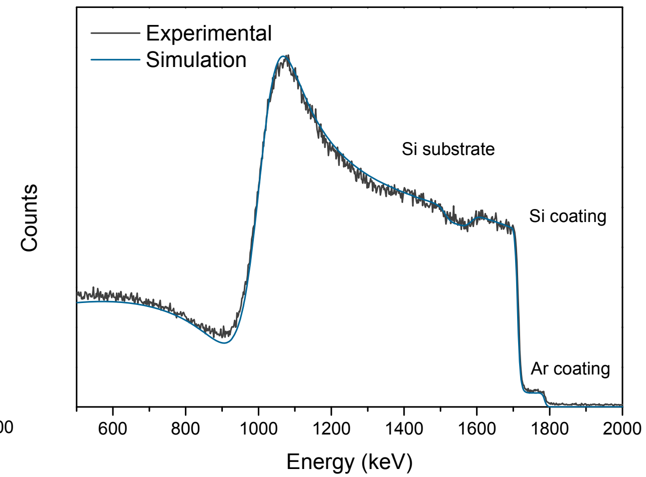

Sample	thickness (10^{15}at/cm^2)	Si (%at)	He (%at)	Ar (%at)
porous	11000	78.7	21.3	--
dense	9500	92.0	--	6.0

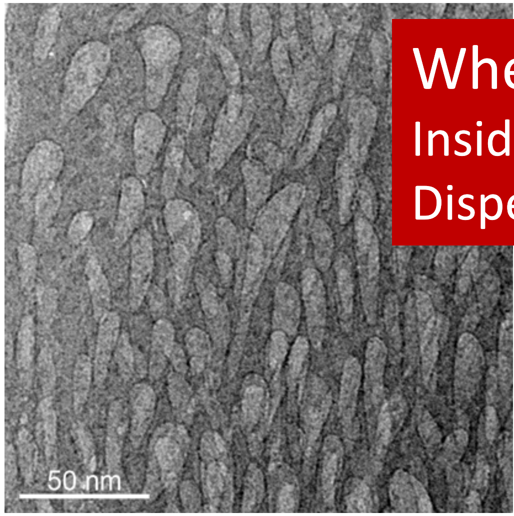

Where is He?
Inside the pores?
Dispersed?

He insolubility in metals is well known

High power and high pressure to increase pore size

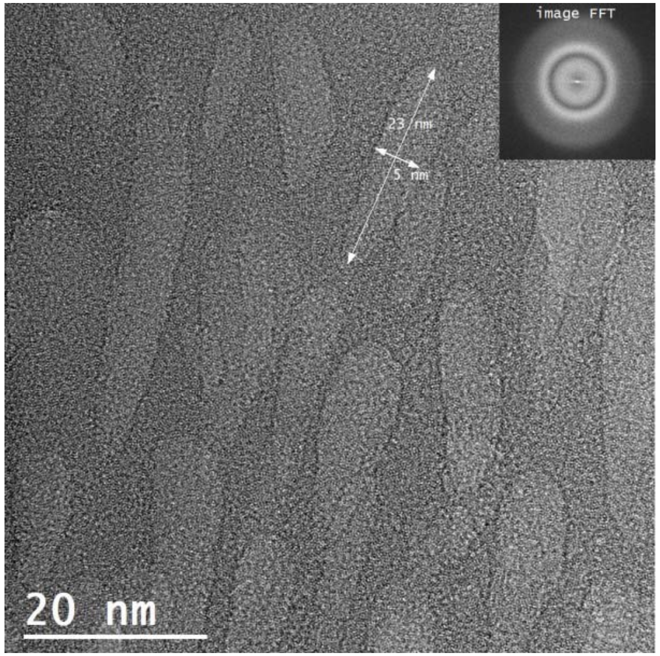

300W rf
4.8Pa He

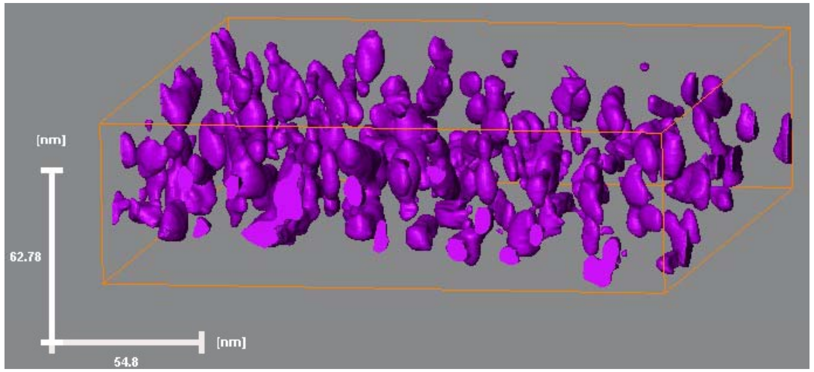

Need of **spatially resolved** analytical tools to be abble to measure **He** signal **inside** and **outside** the pores

STEM-EELS

EELS spectra at various (i,j) positions of the sample. STEM-EELS spectrum images were recorded in the low loss range with a pixel size of 1 nm

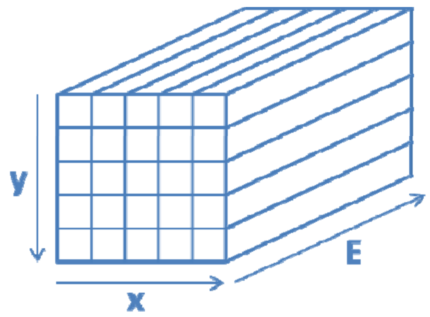

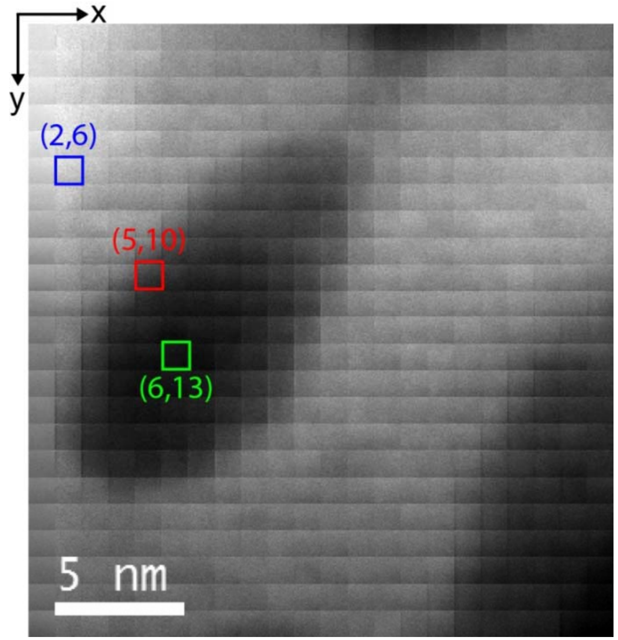

HAADF image – Z contrast

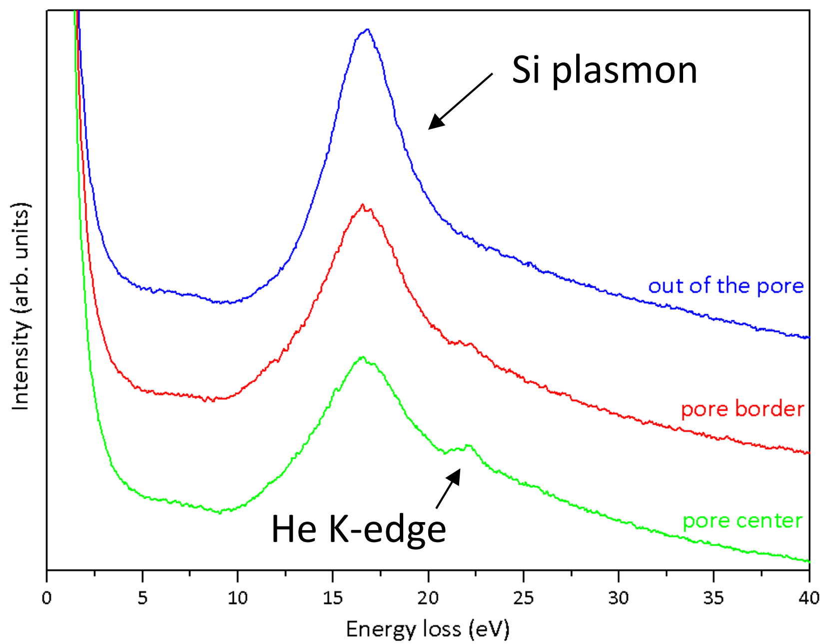

See more details at poster nº75
"Characterization of amorphous and porous silicon coatings by (S)TEM and EELS"

New bottom up method for the production of amorphous **porous silicon** coatings with **closed porosity** by magnetron sputtering

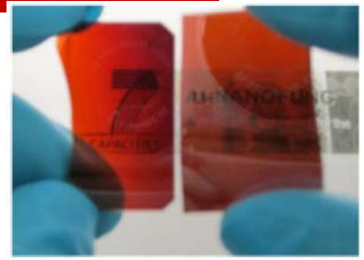

1st bottom up method with closed porosity

- Versatility of magnetron sputtering technique allows to produce coatings with **closed porosity** by depositing directly on large areas

- Depositing on different kinds of substrates like **glass** or even **sensible and flexible substrates** like polymers
- The closed porosity **avoids** the **aging drawbacks** due to exposition to air
- The **refractive index** of the coatings can be easily **changed** by controlling porosity
- Direct deposition of **multilayers** alternating **dense** and **porous** materials just by changing the deposition gas

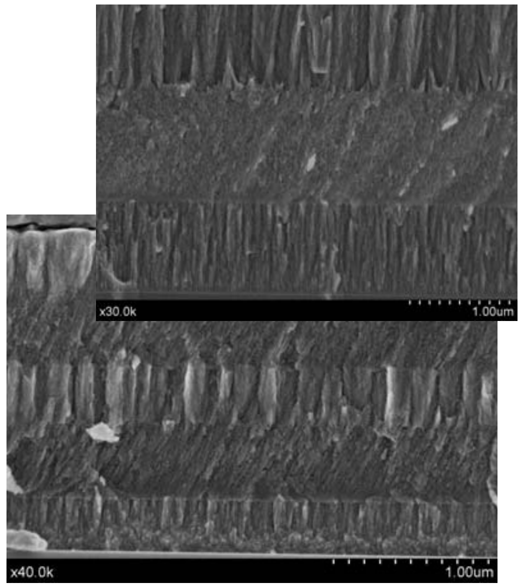

- Deposition of intrinsic or doped silicon

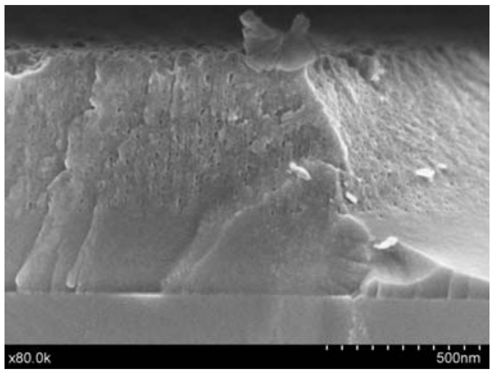

Functional: Electrical and optical

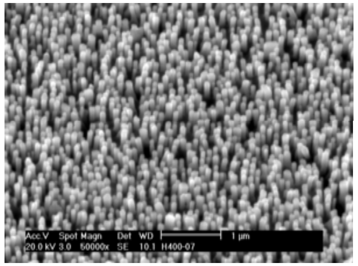

vertically aligned ZnO Nanowires. Transparent & conductive coatings

Thin film Photovoltaic

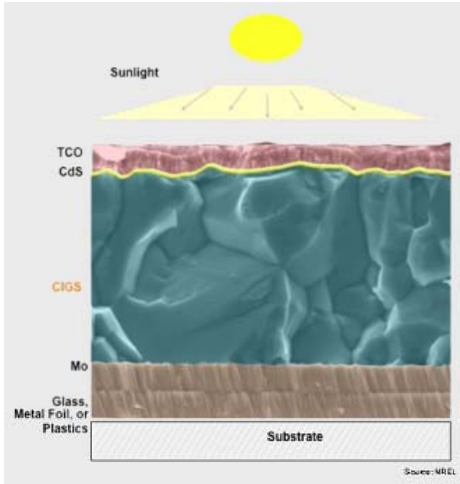

Transparent Conductive Electrodes

EMPA
Materials Science & Technology

Applications of transparent conductive oxides (TCOs)

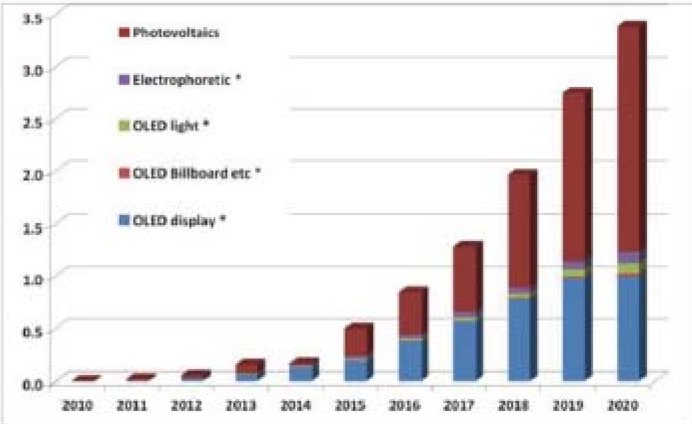

Source: IDTechEX

New applications: High flexible electronics (Prototypes of flexible computers (2013))

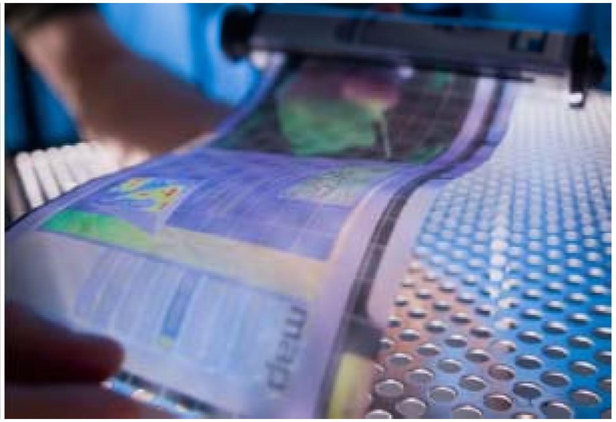

..... requires a replacement of TCOs. → Graphene is an excellent candidate!

Copper indium gallium selenide ($CuIn_xGa_{1-x}Se_2$ or CIGS) is a direct band-gap semiconductor useful for the manufacture of **solar cells**. Because the material has a high absorption coefficient and strongly absorbs sunlight, a much thinner film is required than of other semiconductor materials. Devices made with CIGS belong to the **thin-film** category of photovoltaic's (PV).

CIGS films can be manufactured by different methods:
The most common vacuum-based process is to **co-evaporate or co-sputter copper, gallium, and indium** onto a substrate at room temperature, then anneal the resulting film with a selenide vapor to form the final CIGS structure. An alternative process is to co-evaporate copper, gallium, indium and selenium onto a heated substrate.

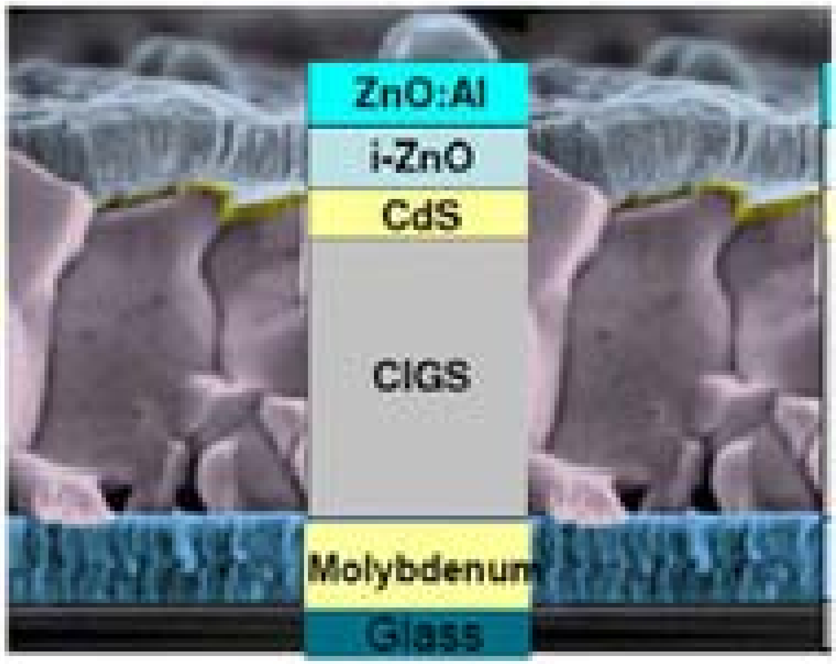

Catalytic coatings, self-cleaning

Co catalysts for H_2 generation

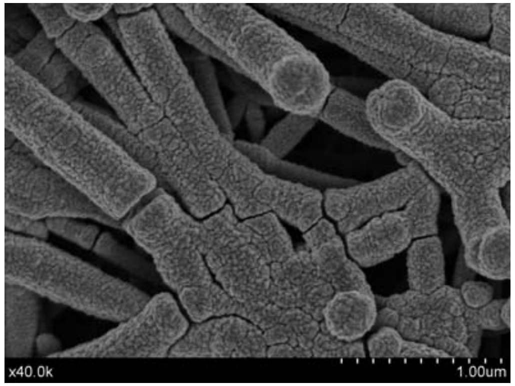

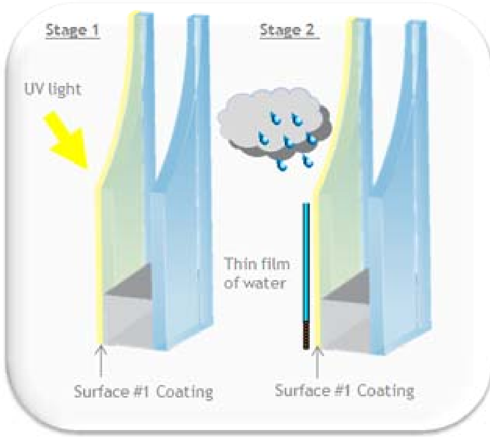

TiO2 based self-cleaning coating

Photoatalytic thin Films

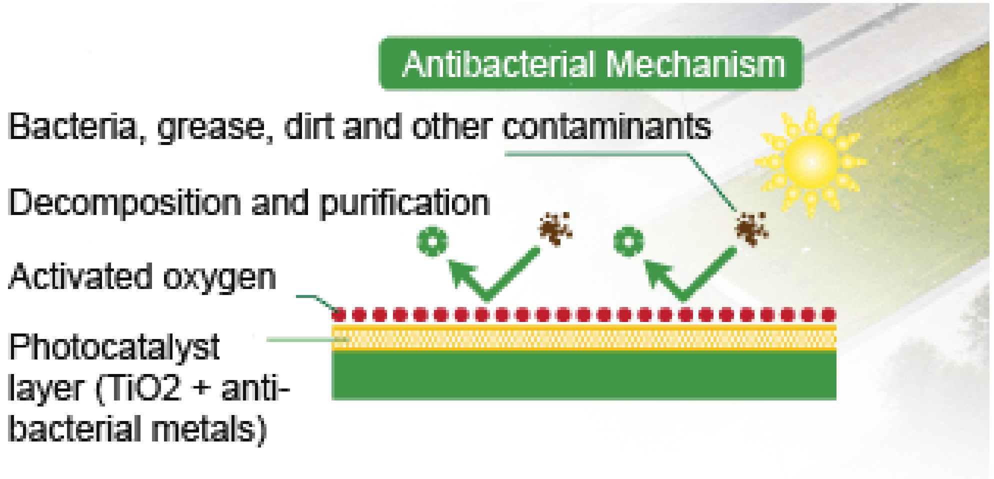

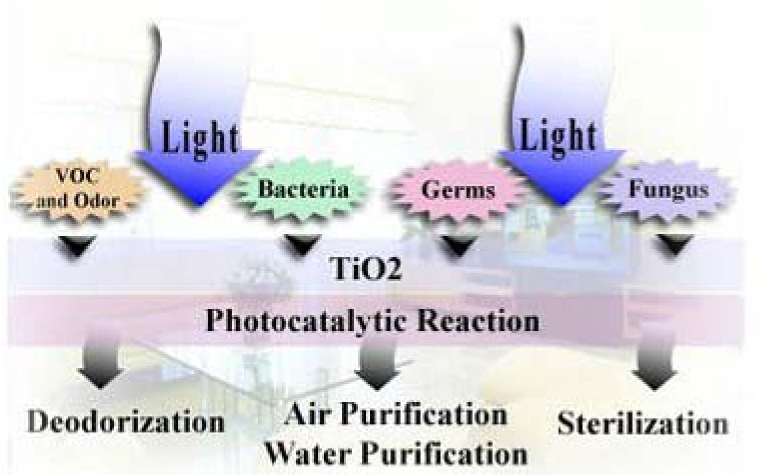

Heterogeneous photocatalysis

Oxidative reactions due to photocatalytic effect:

$$UV + MO \rightarrow MO\ (h + e^{-})$$

Here MO stands for metal oxide ---

$$h^{+} + H_2O \rightarrow H^{+} + \bullet OH$$

$$2\ h^{+} + 2\ H_2O \rightarrow 2\ H^{+} + H_2O_2$$

$$H_2O_2 \rightarrow HO\bullet + \bullet OH$$

The reductive reaction due to photocatalytic effect:

$$e^{-} + O_2 \rightarrow \bullet O_2^{-}$$

$$\bullet O_2{-} + HO\bullet 2 + H^{+} \rightarrow H_2O_2 + O_2$$

$$HOOH \rightarrow HO\bullet + \bullet OH$$

How self-cleaning glass works

Innovative photo-catalytic and hydrophilic coatings based on TiO_2 work in two stages

The unique dual-action self-cleaning coating is located on the external glass panel.

It has got photo-catalytic and hydrophilic properties, and works in two stages:

- (Stage 1)The coating reacts with natural daylight to break down and loosen organic dirt
- (Stage 2) When it rains, instead of forming droplets, the water spreads evenly over the surface of the glass, forming a thin film and helping to wash away any dirt and reduce streaks.

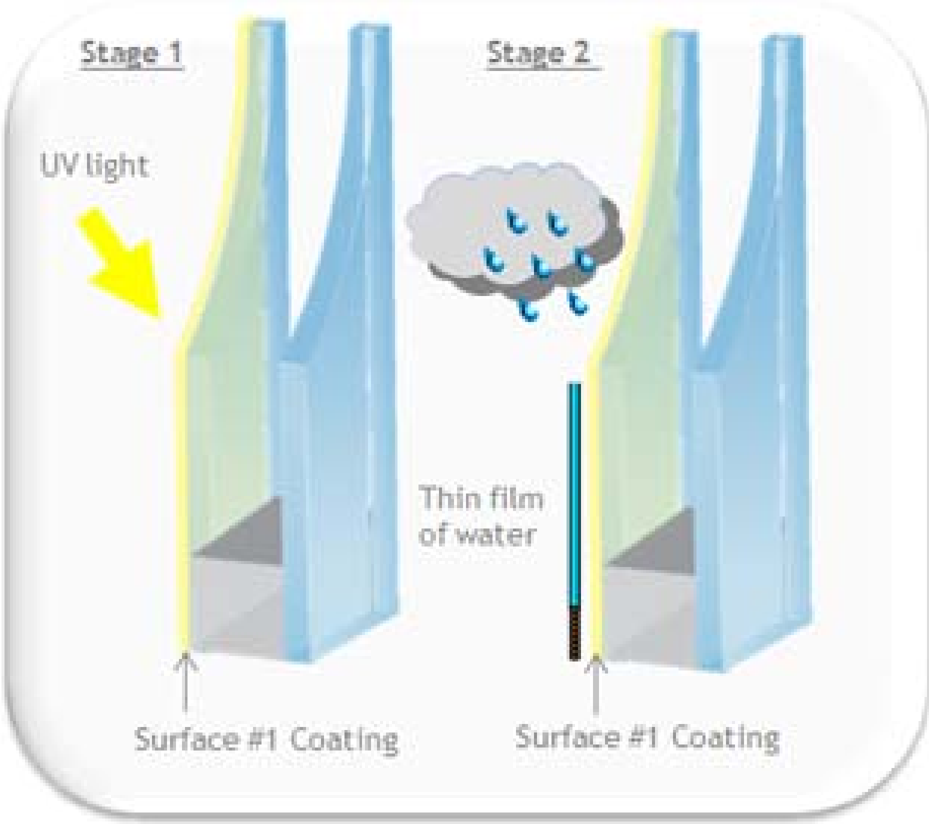

During long dry spells the glass can be cleaned by simply hosing it down with clean water.

TiO_2 can be deposited by reactive magnetron sputtering from Ti target. But also from dip-coatings methodologies from the hydrolysis of Ti-isopropoxide precursors.

Hydrogen storage by $NaBH_4$

$$NaBH_4 + 2\ H_2O \xrightarrow[\text{Catalyst}]{} 4\ H_2 + NaBO_2, \qquad \Delta H < 0$$

It is a safe hydrolysis reaction for hydrogen production in portable applications. The process is controled by a catalysts.

Development of **catalytic membranes** depositing Co-based catalysts by magnetron sputtering

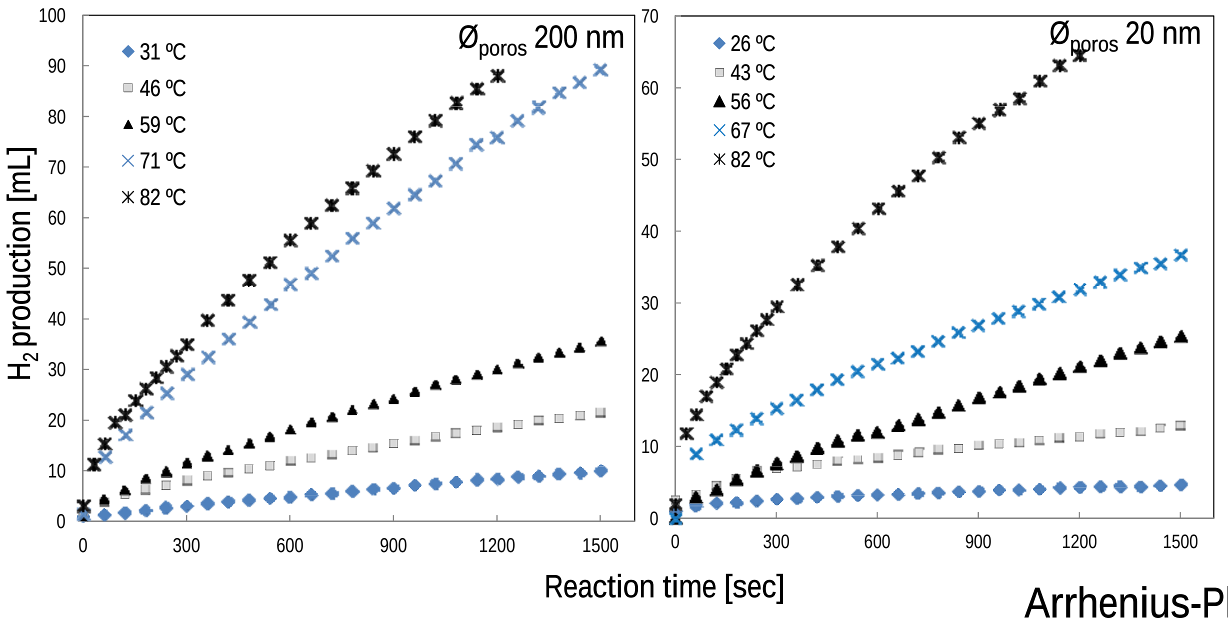

Arrhenius-Plot:

E_A $Ø_{poros}$ 200 nm = 968,9 J/mol

E_A $Ø_{poros}$ 20 nm = 951,8 J/mol

Catalytic membranes

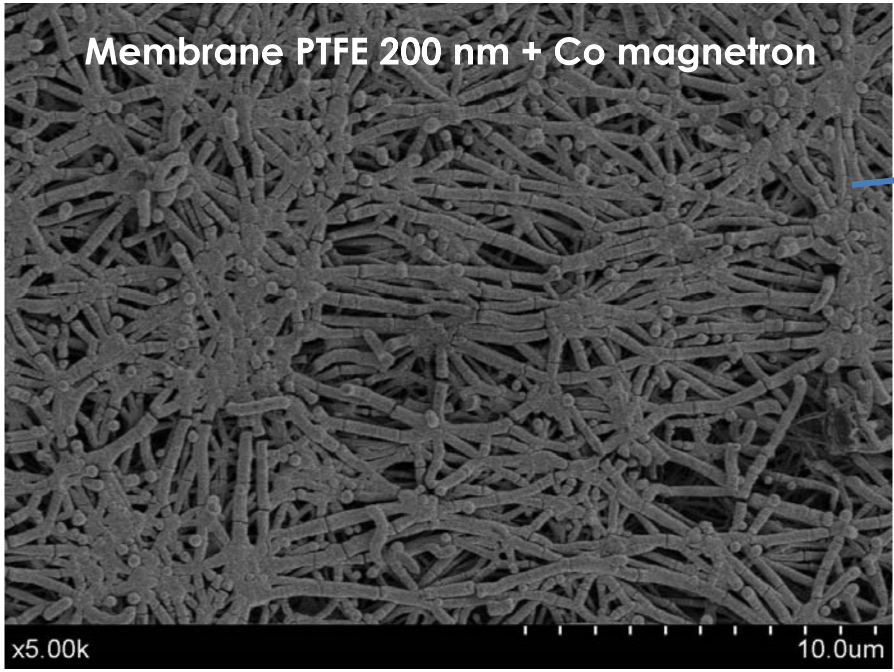

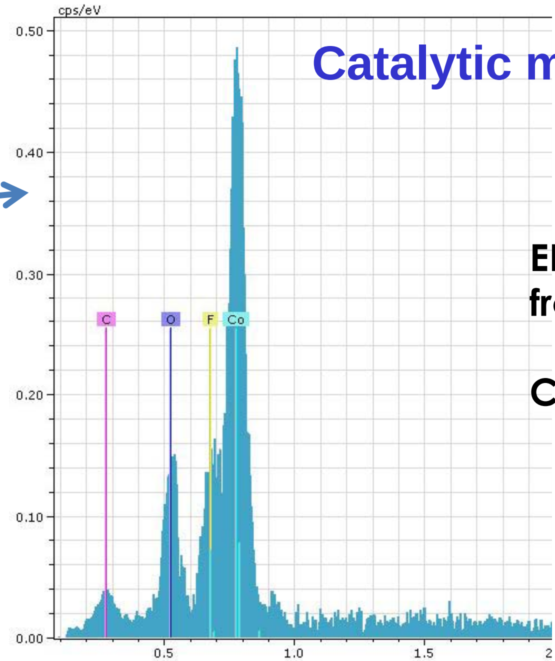

EDS: C and F from PTFE.

Co catalysts

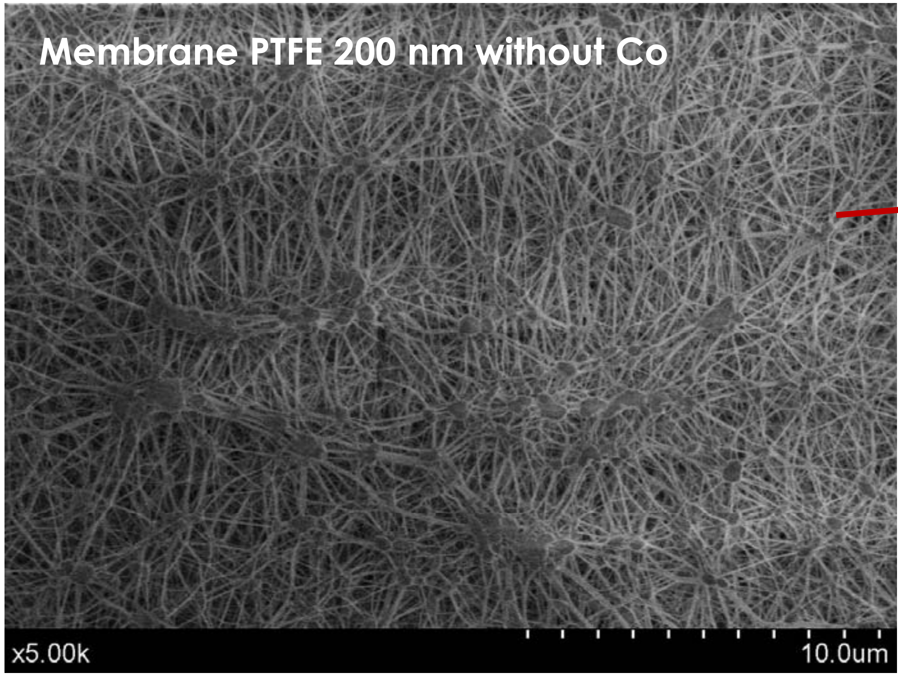

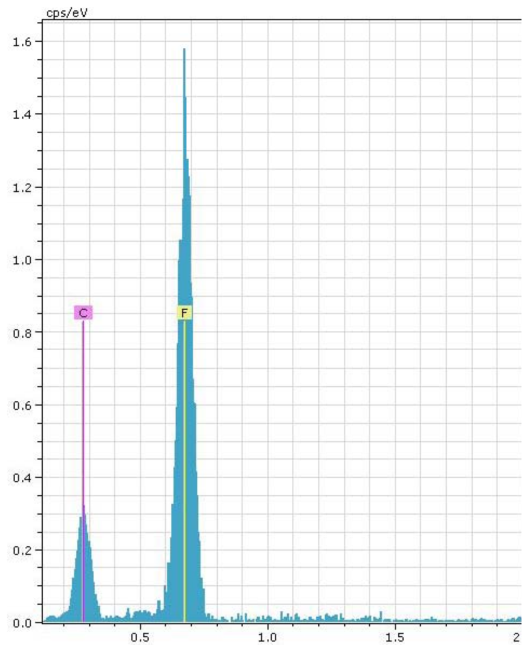

“Magnetron Sputtering” operated at high pressure

The process leads to more granulated or even powdered like materials. Magnetron coupled to a screaper device. Powder is collected below and compacted. Gas phase condensation. Formation of particles in the plasma gas phase by nucleation and growth

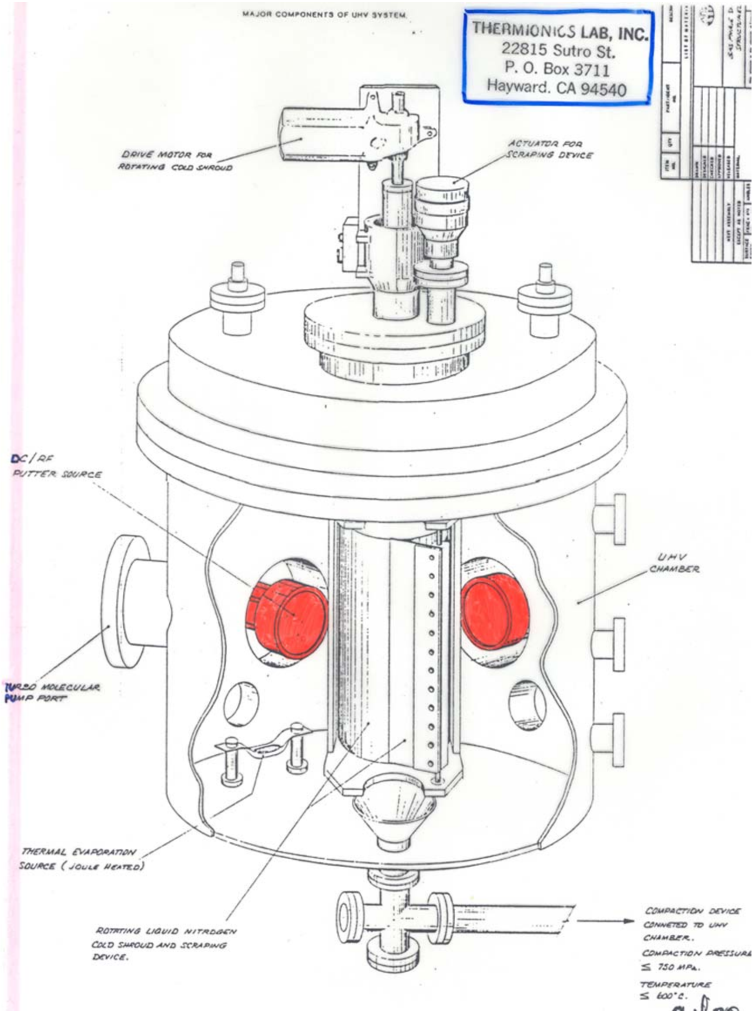

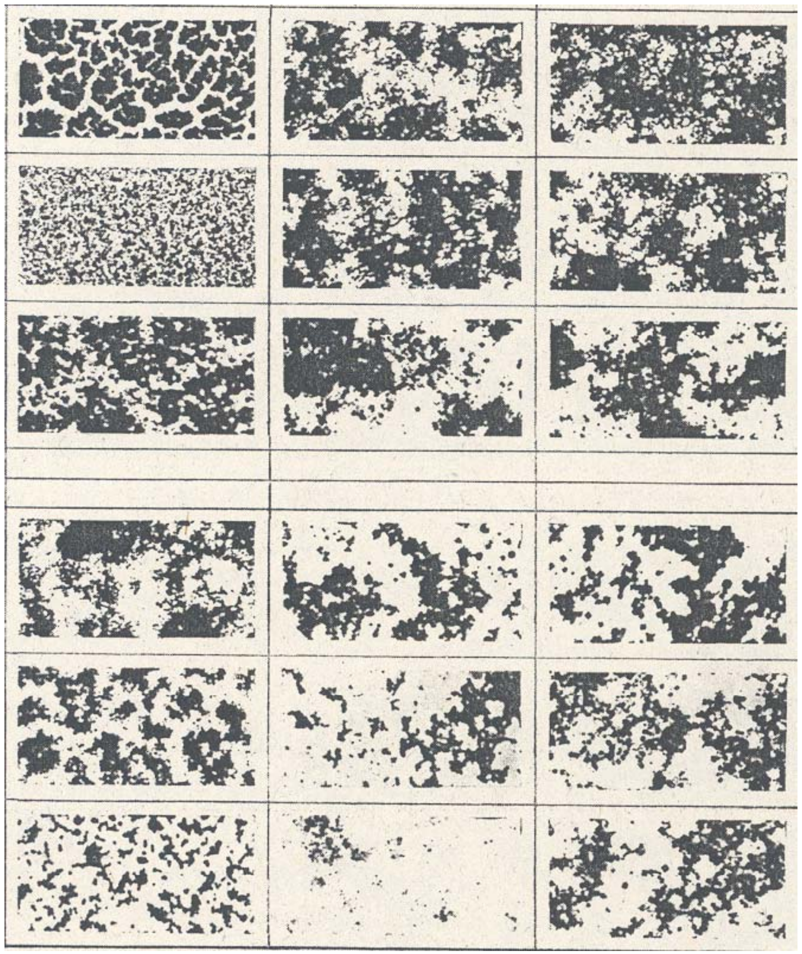

“Cluster source”

A sputtering source for “evaporating” the material from the target

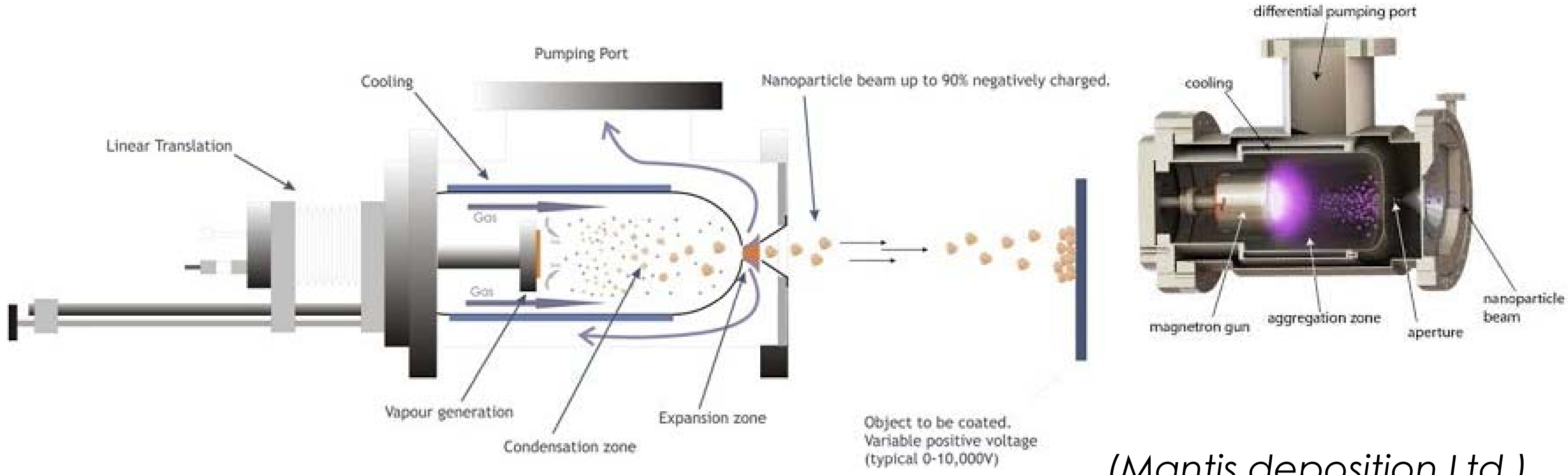

(Mantis deposition Ltd.)

“Terminated cluster growth” is a physical vapor deposition technique that allows fabrication of metallic and conducting oxide nanoparticles with a very narrow size distribution. This type of source operates on the principle of quenching a hot metal vapor in a flowing stream of cool inert gas. The supersaturated vapor cools down due to frequent collisions with inert gas atoms, which leads to condensation and formation of clusters and nanoparticles.

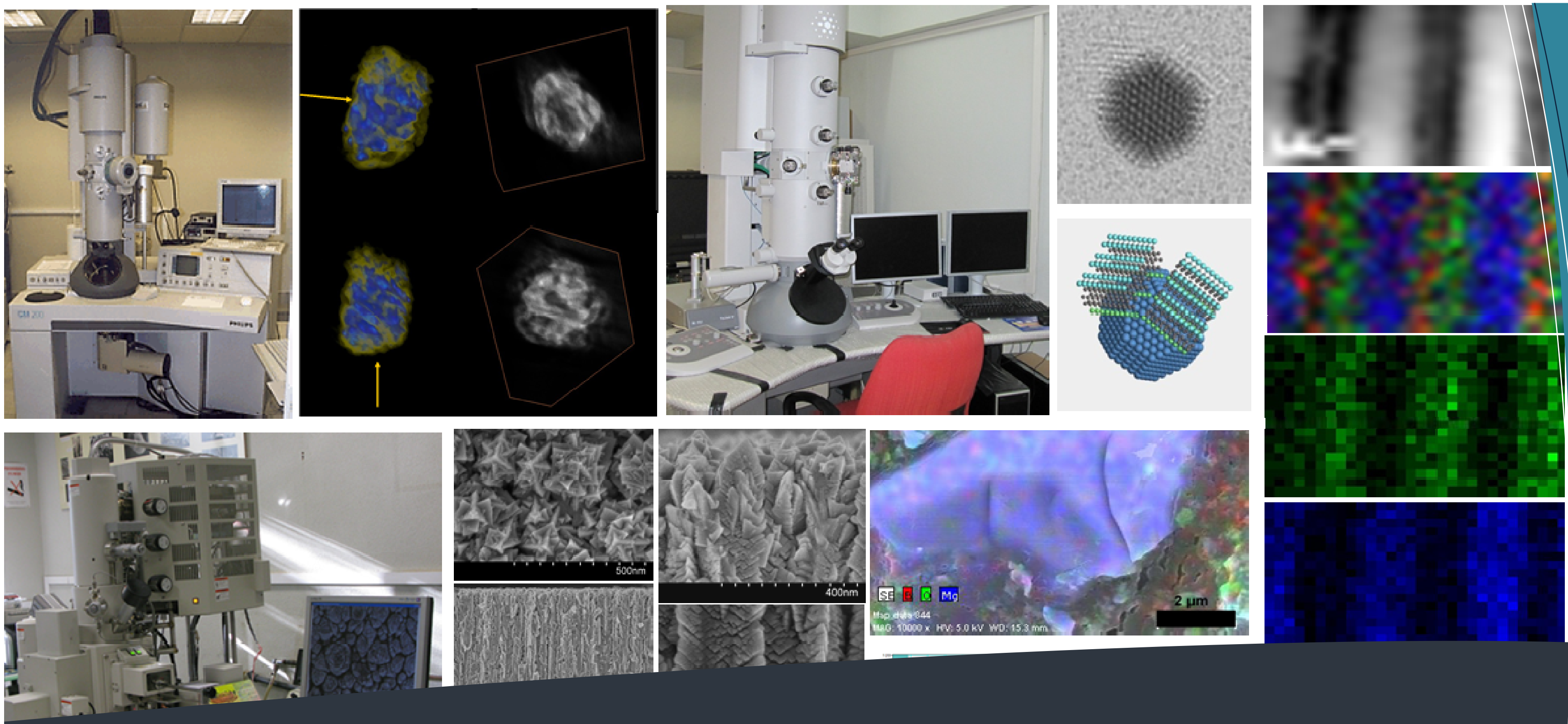

LANE

Laboratorio Avanzado de Nanoscopias y Espectroscopias

AI-NANOFUNC
Advanced Laboratory for the NANO-Analisys of novel FUNCtional Materials
CAPACITIES

JUNTA DE ANDALUCIA

CSIC